Probability Theory of Electron–Molecule, Ion–Molecule, Molecule–Molecule, and Coulomb Collisions for Particle Modeling of Materials Processing Plasmas and Gases

Kenichi Nanbu, *Member, IEEE*

Invited Review

Abstract—The use of high plasma density and low gas density, a recent trend in plasma-assisted materials processing, requires a particle simulation method for plasmas and gas flows. The kinetic theory basis of the particle simulation method is first described. Based on this theoretical viewpoint, state-of-the-art probabilistic treatments of collisions are described for electron–molecule, ion–molecule, molecule–molecule, and Coulomb collisions.

Index Terms—Collision algorithm, direct simulation Monte Carlo (DSMC), materials processing, particle-in-cell (PIC), particle model, plasma, probability theory, rarefied gas.

I. INTRODUCTION

THE USE of high plasma density and low gas pressure is a recent trend in plasma-assisted materials processing, and plasma sources other than capacitively coupled radiofrequency discharge, namely, methods based on inductive coupling, helicon waves, or surface waves, have been developed. The above-mentioned low gas pressure means that the collision frequencies between electron–molecule, ion–molecule, and molecule–molecule are insufficient to recover the equilibrium in velocity distributions of these species; in some cases, the velocity distributions largely deviate from the Maxwellian distribution. If the non-Maxwellian feature of electron energy distribution is disregarded, the ionization rate constant will be underestimated, and hence, the discharge sustaining condition will be inaccurately estimated. Furthermore, if the nonequilibrium of the velocity distribution of molecules or radicals is disregarded, the number flux of these species onto an etched surface and, hence, the etching rate obtained are not reliable. On the other hand, the high plasma density means that Coulomb collisions play an important role in processing plasmas; namely, they influence the electron energy distribution function that governs the ionization rate constant.

Particle modeling, which can be shown to be equivalent to solving the Boltzmann equation, is required to analyze physical or chemical phenomena in low-pressure plasma reactors. Particle modeling has another advantage not possessed by the continuum modeling of plasmas and gas flows. The velocity distribution functions of ions, radicals, or molecules that are incident on an etched wafer can be calculated by means of particle modeling. These distribution functions are indispensable for the prediction of the etched profile of contact holes or trenches on the wafer. Many researchers have conducted one-dimensional (1-D) and two-dimensional (2-D) particle simulations on ordinary desktop computers. In addition, there are various ways of accelerating particle simulations by one or even two orders of magnitude with or without using parallel schemes [1]. Also, with the availability of faster and cheaper workstations, particle simulations, which work from first principles with a minimum of assumptions and approximations, are becoming more attractive.

The particle simulation method has been studied separately by two types of researchers. Plasma physicists, who are concerned with the simulation of charged particles, have developed the particle-in-cell (PIC) method based on the theory of charge assignment and force interpolation. This important theory has made it possible to obtain smooth distributions of charge density and current density in Maxwell's equation of electromagnetic fields. The details of the PIC method can be found in Birdsall and Langdon's book [2], Hockney and Eastwood's book [3], and Birdsall's review [4]. Birdsall [4] also discussed the algorithms for electron–atom and electron–ion collisions. The PIC method, including the Monte Carlo treatment of collisions, is called the PIC/MC method. On the other hand, aerodynamicists have been devoted to developing a particle simulation method of neutral species since the pioneering work of Bird [5], [6]. This method is called the direct simulation Monte Carlo (DSMC) method.

Particle simulation of both charged and neutral species is necessary to examine the structures of plasmas and flows in materials processing, and thus, use of the schemes elaborated on the PIC and DSMC methods is necessary. The purpose of this review is to present a state-of-the-art probabilistic treatment of many types of collisions appearing in plasma processing, such as electron–molecule, ion–molecule, molecule–molecule, Coulomb, and charge–neutralizing collisions. This review is written from the point of view that any probability law used in

particle simulation may be derived from a relevant Boltzmann equation.

II. THEORETICAL BASIS OF PARTICLE SIMULATION

A. The Boltzmann Equation

The theoretical basis of particle simulation is explained using a weakly ionized plasma consisting of electrons (e), ions (A), and molecules (B) as an example. If Coulomb collisions e–e, e–A, and A–A can be disregarded, we have only to consider e–B, A–B, and B–B collisions. The particle motions of species e, A, and B are governed by the respective Boltzmann equations for these species e, A, and B. Except for Coulomb collisions, the Boltzmann equation for electrons or ions is linear, but the Boltzmann equation for molecules is nonlinear because of B–B collisions. Although the PIC/MC method was developed for charged species and the DSMC method was devised for neutral species, the basic idea underlying the two methods is similar. To explain this idea, let us consider the Boltzmann equation of ions A:

$$\frac{\partial f_A}{\partial t} + v_j \frac{\partial f_A}{\partial x_j} + \frac{1}{m_A}\frac{\partial}{\partial v_j}(F_j f_A)$$
$$= \iint [f_A(\boldsymbol{v'})f_B(\boldsymbol{w'}) - f_A(\boldsymbol{v})f_B(\boldsymbol{w})]\, g\sigma^{AB}\, d\Omega\, d\boldsymbol{w}. \quad (1)$$

Here, Coulomb collisions are disregarded and only A–B collisions are taken into consideration, summation over repeated suffix j is implied, F_j is the force acting on particle A with a mass of m_A, $f_A(\boldsymbol{v})$ and $f_B(\boldsymbol{w})$ are the velocity distribution functions of species A and B, $\boldsymbol{v'}$ and $\boldsymbol{w'}$ are the postcollision velocities, $g = |\boldsymbol{v} - \boldsymbol{w}|$ is the relative speed, σ^{AB} is the differential cross section, and $d\Omega (= \sin\chi\, d\chi\, d\psi)$ is the solid angle. For the sake of simplicity, $f_A(\boldsymbol{v}, \boldsymbol{x}, t)$ and $f_B(\boldsymbol{w}, \boldsymbol{x}, t)$ are expressed as $f_A(\boldsymbol{v})$ and $f_B(\boldsymbol{w})$ in the right-hand side. The differential cross section σ^{AB} is a function of g and the deflection angle χ. The force $\boldsymbol{F}$ is given by

$$\boldsymbol{F} = q_A(\boldsymbol{E} + \boldsymbol{v} \times \boldsymbol{B}), \quad (2)$$

where q_A is the charge of particle A and $\boldsymbol{E}$ and $\boldsymbol{B}$ are the electric and magnetic fields, respectively.

If the method to obtain $f_A(\boldsymbol{v}, \boldsymbol{x}, t + \Delta t)$ from a known $f_A(\boldsymbol{v}, \boldsymbol{x}, t)$ is given, the solution f_A can be found at any time by step-by-step calculations started from an initial velocity distribution function. For a small Δt, we have

$$f_A(\boldsymbol{v}, \boldsymbol{x}, t + \Delta t) = f_A(\boldsymbol{v}, \boldsymbol{x}, t) + \Delta t \left(\frac{\partial f_A}{\partial t}\right)_t. \quad (3)$$

Substitution of $\partial f_A/\partial t$ of (1) into (3) yields

$$f_A(\boldsymbol{v}, \boldsymbol{x}, t + \Delta t) = (1 + \Delta t J)(1 + \Delta t D) f_A(\boldsymbol{v}, \boldsymbol{x}, t) \quad (4)$$

where D and J are operators defined by

$$D(f_A) = -v_j \frac{\partial f_A}{\partial x_j} - \frac{1}{m_A}\frac{\partial}{\partial v_j}(F_j f_A) \quad (5)$$

$$J(f_A) = \iint [f_A(\boldsymbol{v'})f_B(\boldsymbol{w'}) - f_A(\boldsymbol{v})f_B(\boldsymbol{w})]\, g\sigma^{AB}\, d\Omega\, d\boldsymbol{w}. \quad (6)$$

Clearly, D and J denote noncollisional and collisional operators, respectively, and hence, (4) represents decoupling of noncollisional and collisional parts of the motion. Equation (4) is equal to (3) if the term of order $(\Delta t)^2$ is disregarded; i.e., the solution obtained from (4) is first-order accurate. As is discussed later, in general, Δt should be much less than the mean free time τ (mean free path divided by mean speed of particle). This condition should be strictly satisfied in the case when particle A is a charged particle [7]. Note, however, that if particle A is a molecule, the condition can be replaced by a weaker one of $\Delta t < \tau$. The reason why the weaker condition is practically applicable is probably that molecular trajectories are straight and, hence, accurate for any Δt and that the state of gas changes little in the mean free time.

Equation (4) suggests a method of solving the Boltzmann equation: first, obtain $f_A^* \equiv (1 + \Delta t D) f_A$ and then obtain $(1 + \Delta t J) f_A^*$. The function f_A^* is the noncollisional part of the solution. The first procedure is equivalent to solving

$$\frac{\partial f_A}{\partial t} + v_j \frac{\partial f_A}{\partial x_j} + \frac{1}{m_A}\frac{\partial}{\partial v_j}(F_j f_A) = 0 \quad (7)$$

by use of the initial distribution function $f_A(\boldsymbol{v}, \boldsymbol{x}, t)$. Let the solution at $t + \Delta t$ be $f_A^*(\boldsymbol{v}, \boldsymbol{x}, t)$. The solution is $f_A^*(\boldsymbol{v}, \boldsymbol{x}, t) = f_A(\boldsymbol{v} - (\boldsymbol{F}/m_A)\Delta t, \boldsymbol{x} - \boldsymbol{v}\Delta t, t)$, and hence

$$f_A^*(\boldsymbol{v} + \Delta \boldsymbol{v}, \boldsymbol{x} + \Delta \boldsymbol{x}, t) = f_A(\boldsymbol{v}, \boldsymbol{x}, t) \quad (8)$$

where $\Delta \boldsymbol{v} = (\boldsymbol{F}/m_A)\Delta t$ and $\Delta \boldsymbol{x} = \boldsymbol{v}\Delta t$. Equation (8) simply means that the particles of species A move according to the equation of motion

$$m_A \frac{d\boldsymbol{v}}{dt} = q_A(\boldsymbol{E} + \boldsymbol{v} \times \boldsymbol{B}) \quad (9a)$$

$$\frac{d\boldsymbol{x}}{dt} = \boldsymbol{v}. \quad (9b)$$

The equation of motion is used in PIC simulations, which means that the Boltzmann equation without the collision term is solved by the PIC. (Using finite-sized particles in the PIC means that Coulomb collisions, correct at range greater than a cell size, are taken into consideration.) When (9a) and (9b) are solved for all particles, we have $f_A^*(\boldsymbol{v}, \boldsymbol{x}, t)$. The second procedure is equivalent to solving

$$\frac{\partial f_A}{\partial t} = \iint [f_A(\boldsymbol{v'})f_B(\boldsymbol{w'}) - f_A(\boldsymbol{v})f_B(\boldsymbol{w})]\, g\sigma^{AB}\, d\Omega\, d\boldsymbol{w} \quad (10)$$

by use of the initial distribution function $f_A^*(\boldsymbol{v}, \boldsymbol{x}, t)$. The solution of (10) at $t + \Delta t$ is $f_A(\boldsymbol{v}, \boldsymbol{x}, t + \Delta t)$.

Equation (10), which does not include the term $\partial f_A/\partial x_j$, represents the collisional relaxation of the velocity distribution in a spatially uniform state of species A; (10) can be applied only to a small cell where the gradient of density, temperature, and flow velocity of species A can be regarded as being uniform. The dimension of the cell should be the order of the mean free path of species A. Note, however, that this is true in the case of no electric or magnetic field. In simulations of plasma discharges, it is necessary to resolve the sheath where the gradient

of electron and ion densities is very large. In such cases, the dimension of the cell should be much smaller than is the sheath thickness, which is the order of the Debye length. Therefore, if the Debye length is shorter than is the mean free path, the dimension of the cell should be a fraction of the Debye length. This is the reason why the computational domain should be divided into small cells in the PIC and DSMC methods. Equation (10) can be solved by use of an equivalent stochastic process [8]. The essential idea is as follows. First, we note that in particle simulation, it is sufficient to consider the motions of a set of particles randomly sampled from all particles. The sampled particles are called simulated particles. The sampling is done only once at time zero, and every simulated particle with a given name is followed for its lifetime. The number of simulated particles in a cell is much smaller than is the number of real particles. Let W be the ratio of the number of real particles to that of simulated particles. The factor W is called weight. Here, the change of the attribute of the simulated particle is necessary to conserve charge, mass, momentum, and energy in a system of real particles; the charge and mass of the simulated particle are multiplied by W. The resulting particle is called superparticle in PIC. Because the charge to mass ratio of the superparticle is the same as that of the real particle, the equation of motion for the superparticle coincides with that of the real particle. Because there is no fear of confusion, hereafter the superparticle is called simulated particle (with the weight). After moving all simulated particles by Δt, we identify the simulated particles in each cell by examining the positions of the particles. Let N_A be the number of simulated particles in a cell and $\boldsymbol{v}_{A1}, \boldsymbol{v}_{A2}, \ldots$ be the particle velocities. The velocity distribution function $f_A^*(\boldsymbol{v}, \boldsymbol{x}, t)$ for a cell located at $\boldsymbol{x}$ is expressed as

$$f_A^*(\boldsymbol{v}, \boldsymbol{x}, t) = \frac{n_A}{N_A} \sum_{i=1}^{N_A} \delta^3(\boldsymbol{v} - \boldsymbol{v}_{Ai}) \tag{11}$$

where

n_A number density for the cell;
$\delta^3(\ )$ delta function;
$\boldsymbol{v}_{Ai}$ solution of (9a) at time $t + \Delta t$.

The function $\delta^3(\boldsymbol{v} - \boldsymbol{v}_{Ai})$ is the probability density function for the velocity $\boldsymbol{v}_{Ai}$ of particle Ai. Similarly, the velocity distribution function of species B at the end of the particle's motion is

$$f_B^*(\boldsymbol{w}, \boldsymbol{x}, t) = \frac{n_B}{N_B} \sum_{j=1}^{N_B} \delta^3(\boldsymbol{w} - \boldsymbol{v}_{Bj}) \tag{12}$$

where $\boldsymbol{v}_{Bj}$ is the velocity of simulated particle Bj. Note that $\boldsymbol{v}_{Bj}$ is constant because the external force is null for neutral species B. The solution $f_A(\boldsymbol{v}, \boldsymbol{x}, t + \Delta t)$ can be obtained from

$$
\begin{aligned}
&f_A(\boldsymbol{v}, \boldsymbol{x}, t + \Delta t) \\
&= (1 + \Delta t J) f_A^*(\boldsymbol{v}, \boldsymbol{x}, t) \\
&= f_A^*(\boldsymbol{v}, \boldsymbol{x}, t) + \Delta t \iint \\
&\quad \cdot [f_A^*(\boldsymbol{v}') f_B^*(\boldsymbol{w}') - f_A^*(\boldsymbol{v}) f_B^*(\boldsymbol{w})] g\sigma^{AB} \, d\Omega \, d\boldsymbol{w}. \tag{13}
\end{aligned}
$$

Substitution of (11) and (12) into (13) yields, after lengthy manipulation

$$f_A(\boldsymbol{v}, \boldsymbol{x}, t + \Delta t) = \frac{n_A}{N_A} \sum_{i=1}^{N_A} f_{Ai}(\boldsymbol{v}) \tag{14}$$

where $f_{Ai}(\boldsymbol{v})$ is the probability density function for the velocity of particle Ai at $t + \Delta t$. It is given by

$$f_{Ai}(\boldsymbol{v}) = (1 - P_{Ai})\delta^3(\boldsymbol{v} - \boldsymbol{v}_{Ai}) + P_{Ai}Q_{Ai}(\boldsymbol{v}). \tag{15}$$

The structure of (15) states that P_{Ai} is the collision probability of particle Ai. Note that if $P_{Ai} = 0$, $f_{Ai}(\boldsymbol{v}) = \delta^3(\boldsymbol{v} - \boldsymbol{v}_{Ai})$, i.e., there is no change in velocity due to a collision. The probability P_{Ai} is given by

$$P_{Ai} = \sum_{j=1}^{N_B} P_{Ai, \, Bj} \tag{16}$$

where

$$P_{Ai, \, Bj} = N_B^{-1} n_B g_{Ai, \, Bj} \sigma_T^{AB}(g_{Ai, \, Bj}) \Delta t. \tag{17}$$

Here, $g_{Ai, \, Bj} = |\boldsymbol{v}_{Ai} - \boldsymbol{v}_{Bj}|$ is the relative speed and σ_T^{AB} is the total collision cross section. Equation (16) reveals that $P_{Ai, \, Bj}$ is the probability of particle Ai colliding with particle Bj in Δt. The function $Q_{Ai}(\boldsymbol{v})$ is the probability density function for the postcollision velocity $\boldsymbol{v}$. It is written as

$$Q_{Ai}(\boldsymbol{v}) = \sum_{j=1}^{N_B} \frac{P_{Ai, Bj}}{P_{Ai}} Q_{Ai, Bj}(\boldsymbol{v}). \tag{18}$$

Here, the ratio $P_{Ai, Bj}/P_{Ai}$ represents the conditional probability that the collision partner of particle Ai is particle Bj under the condition that particle Ai collides in Δt. Now, the meaning of $Q_{Ai, Bj}(\boldsymbol{v})$ is clear: $Q_{Ai, Bj}(\boldsymbol{v})$ is the probability density function for the postcollision velocity of particle Ai when its collision partner is particle Bj. It is given by

$$Q_{Ai, Bj}(\boldsymbol{v}) = \frac{\sigma^{AB}(g_{Ai, Bj}, \chi)\delta(|\boldsymbol{g}'| - g_{Ai, Bj})}{(g_{Ai, Bj})^2 M_B^3 \sigma_T^{AB}(g_{Ai, Bj})} \tag{19}$$

where

$$\boldsymbol{g}' = \frac{1}{M_B}(\boldsymbol{v} - M_A \boldsymbol{v}_{Ai} - M_B \boldsymbol{v}_{Bj}) \tag{20}$$

$M_A = m_A/(m_A + m_B)$, $M_B = m_B/(m_A + m_B)$, χ is the angle between $\boldsymbol{g}'$ and $\boldsymbol{v}_{Ai} - \boldsymbol{v}_{Bj}$, and $\sigma^{AB}(g_{Ai, Bj}, \chi)$ is the differential cross section. From (19), we have

$$
\begin{aligned}
&Q_{Ai, Bj}(\boldsymbol{v}) \, d\boldsymbol{v} \\
&= \delta(|\boldsymbol{g}'| - g_{Ai, Bj}) \, dg' \frac{\sigma^{AB}(g_{Ai, Bj}, \chi) \sin \chi \, d\chi \, d\psi}{\sigma_T^{AB}(g_{Ai, Bj})} \tag{21}
\end{aligned}
$$

where we used $d\boldsymbol{v} = M_B^3 \, d\boldsymbol{g}' = M_B^3 g'^2 \, dg' \sin \chi \, d\chi \, d\psi$. Note that M_B^3 is the Jacobian of the transformation from $\boldsymbol{v}$ to $\boldsymbol{g}'$. Equation (21) determines the magnitude and direction of $\boldsymbol{g}'$, and

hence, (20) yields the postcollision velocity $\boldsymbol{v}'_{Ai}(\equiv \boldsymbol{v})$ of particle Ai

$$\boldsymbol{v}'_{Ai} = \frac{1}{m_A + m_B}(m_A\boldsymbol{v}_{Ai} + m_B\boldsymbol{v}_{Bj} + m_B\boldsymbol{g}') \qquad (22)$$

where $\boldsymbol{g}'(= \boldsymbol{v}'_{Ai} - \boldsymbol{v}'_{Bj})$ is the postcollision relative velocity and $|\boldsymbol{g}'| = g_{Ai,Bj}$. The probability that $\boldsymbol{g}'$ is included in the solid angle $\sin\chi\,d\chi\,d\psi$ is $\sigma^{AB}(g_{Ai,Bj}, \chi)\sin\chi\,d\chi\,d\psi/\sigma_T^{AB}(g_{Ai,Bj})$. The direction (χ, ψ) of $\boldsymbol{g}'$ can be sampled using this probability.

Equations (16) and (17), which are derived from the Boltzmann equation, can also be obtained by use of the elementary free-path theory. The collision frequency of particle Ai is

$$\nu_{Ai} = n_B\overline{g_{Ai,\,B}\sigma_T^{AB}(g_{Ai,\,B})}$$

where $g_{Ai,\,B}$ is the relative speed between Ai and some particle B, and the bar denotes the average of particles B. Let us take the average of all simulated particles B in a cell. Then, the collision probability of particle Ai takes the form

$$P_{Ai} = \nu_{Ai}\Delta t = \frac{n_B\Delta t}{N_B}\sum_{j=1}^{N_B} g_{Ai,Bj}\sigma_T^{AB}(g_{Ai,Bj}).$$

This equation agrees with (16). Of course, we cannot obtain the probability laws to determine the postcollision velocities from the free-path theory. However, in many cases, we can write such probability laws intuitively because the laws derived from the Boltzmann equation agree with our physical image of collision.

The probability laws used to determine the velocity of particle Ai at $t + \Delta t$ are summarized as follows:

1) Particle Ai collides in Δt with a probability of P_{Ai}.
2) Under the condition that particle Ai collides, its collision partner is particle Bj with a probability of $P_{Ai,Bj}/P_{Ai}$; the partner is found from the probability distribution $\{P_{Ai,Bj}/P_{Ai}: j = 1, 2, \ldots, N_B\}$.
3) If the collision partner is Bj, the postcollision velocity $\boldsymbol{v}'_{Ai}$ is given by (22).

We have seen that the particle simulation method can be derived from the Boltzmann equation of ions. This is true for any species. Although the Boltzmann equation for a simple gas is nonlinear because of collisions between like molecules, the simulation method was derived in 1980 by the author [9]. Before the author's work, the particle simulation method had been regarded as a kind of numerical experiment by those in the field of rarefied gas dynamics. By use of the measure theory, mathematicians [10] verified that Nanbu's particle simulation method is an appropriate method for solving the Boltzmann equation.

Under conditions of high plasma density, the velocity distribution of charged particles is affected by Coulomb collisions and the velocity distribution is governed by the Landau–Fokker–Planck equation. The particle simulation method for electrons and ions can be derived from the Landau–Fokker–Planck equation. Rosenbluth *et al.* [11] derived the Landau–Fokker–Planck equation from the Boltzmann equation under the assumption that small-angle Coulomb collisions are much more important than are collisions, resulting in large velocity changes. Rosenbluth *et al.*'s derivation suggests

that a method of simulating Coulomb collisions in plasma can also be derived from the Boltzmann equation. This is discussed in Section III-D-1.

The most important ideas of the particle simulation method can be summarized as 1) decoupling of collisionless motion and collision and 2) calculating collisions independently in each cell. These basic ideas have been shown to naturally result from the operator splitting in the form of $(1+\Delta tJ)(1+\Delta tD)$. Let us consider the conditions for choosing Δt. The operator splitting is allowed if and only if $\Delta t|J(f_A)| \ll f_A$ and $\Delta t|D(f_A)| \ll f_A$. The first condition states that the effect of collision in Δt; must be small; i.e., the collision probability $P_{Ai} \simeq \Delta t/\tau$ is small, where τ is the mean free time; the time step Δt must satisfy the condition $\Delta t \ll \tau$. The second condition $\Delta t|D(f_A)| \ll f_A$ requires that $|\Delta\boldsymbol{x}| \ll |\boldsymbol{x}|$ and $|\Delta\boldsymbol{v}| \ll |\boldsymbol{v}|$ in (8). That is, $\overline{v}\Delta t \ll x$ and $(\overline{F}/m_A)\Delta t \ll \overline{v}$, where $\overline{v}$ is the mean particle speed and $\overline{F}/m_A$ is the mean acceleration. The condition $\overline{v}\Delta t \ll x$ is usually replaced by the Courant condition $\overline{v}\Delta t < \Delta_c$, where Δ_c denotes the cell size: a particle's displacement in Δt must be less than the cell size. The condition $(\overline{F}/m_A)\Delta t \ll \overline{v}$ requires that the change in the particle's speed in Δt must be much less than the original speed; i.e., a smaller Δt should be used for a stronger external field.

B. Self-Consistent Simulation

The solution of the equation-of-motion for molecule i is

$$\boldsymbol{v}_i(t + \Delta t) = \boldsymbol{v}_i(t) \qquad (23a)$$
$$\boldsymbol{x}_i(t + \Delta t) = \boldsymbol{x}_i(t) + \boldsymbol{v}_i(t)\Delta t. \qquad (23b)$$

During the motion in Δt, some molecules are reflected or adsorbed on a wall, some are pumped out to an exit, and some fresh molecules are fed in through an inlet. The change in $\boldsymbol{v}_i$ and $\boldsymbol{x}_i$ because of these causes are considered in the stage of collisionless motion. The change in $\boldsymbol{v}_i$ by molecular collision is considered in the stage of collision. Repetition of the two stages is sufficient for the simulation of neutral species. In the simulation of charged species, we must calculate new $\boldsymbol{E}$ and $\boldsymbol{B}$ fields after the collisionless motion. Maxwell's equations for plasmas are

$$\frac{1}{\mu_0}\nabla \times \boldsymbol{B} = \boldsymbol{j} + \epsilon_0\frac{\partial\boldsymbol{E}}{\partial t} \qquad (24)$$
$$\nabla \times \boldsymbol{E} = -\frac{\partial\boldsymbol{B}}{\partial t} \qquad (25)$$
$$\nabla \cdot \boldsymbol{E} = \frac{\rho}{\epsilon_0} \qquad (26)$$
$$\nabla \cdot \boldsymbol{B} = 0 \qquad (27)$$

where

ϵ_0 and μ_0 permittivity and permeability of free space, respectively;
$\boldsymbol{j}$ current density;
ρ charge density.

Because $\boldsymbol{j}$ is obtained from the data $\{(\boldsymbol{x}_i, \boldsymbol{v}_i): i = 1, 2, \ldots\}$ and ρ is obtained from the data $\{\boldsymbol{x}_i: i = 1, 2, \ldots\}$ of charge particles, equations of motion, (9a) and (9b), are coupled with Maxwell's equations. When the coupling is fully taken into consideration, the simulation is called self-consistent. The overall simulation procedure of charged particles for

one time-step consists of 1) solving equations of motion, 2) calculating collisions, and 3) solving Maxwell's equations. One-dimensional discharge problems have been solved using this procedure [12]–[15]. Stage 3) is, however, time-consuming when E and B fields are axisymmetrical or three-dimensional (3-D). Methods of solving Maxwell's equations are fully discussed by Birdsall and Langdon [2] and Hockney and Eastwood [3].

In direct current magnetron discharges, the external B field is so strong that the induced B field can be disregarded. We then need only solve (26). The Poisson equation for potential ϕ is

$$\nabla^2 \phi = -\frac{\rho}{\epsilon_0}.$$

Nanbu and Kondo [16] carried out self-consistent particle simulation of a 3-D dc magnetron discharge. They solved the 3-D Poisson equation at each electron time-step (0.2 ns) using the fast Fourier transform. Although the computation time was considerable, i.e., a few hundred hours with a 1-Gflops vector computer, the detailed structure of the discharge [16] and even a chaotic dynamics of plasma [17] were found. The most important and urgent necessity in the 3-D PIC simulation is to develop a rapid solver of multidimensional Maxwell's equations and a technique to vectorize the charge assignment routine.

III. MONTE CARLO COLLISION ALGORITHM

Species in argon plasma are electron e, ion Ar^+, metastable atom Ar^*, and ground state atom Ar. Here, Ar^* is disregarded. Fig. 1 shows the types of collisions among these species. The bold lines represent the collisions between neutral atoms, the fine lines represent those between charged particles and neutral atoms, and the dashed lines represent those between charged particles. The dashed line pairs (e–e, e–Ar^+, Ar^+–Ar^+) are subject to a long-range force and result in Coulomb collisions. All other pairs are subject to a short-range force. The collision algorithm for Coulomb collisions is different from the algorithm for the short-range force. In Coulomb collisions, small-angle scatterings are dominant in the transfer of momentum and energy, whereas in the collisions of short-range force, large-angle scatterings are much more important.

The collision algorithms can also be divided into two groups based on another scheme. One is collisions between like particles, and the other is collisions between unlike particles. The collision term of the Boltzmann equation is nonlinear for like collisions and linear for unlike collisions. Consequently, the collision algorithm for like collisions is different from that for unlike collisions. Here, we divide the collision algorithms into three:

1) short-range collisions between unlike particles

   e–Ar, Ar^+–Ar;

2) short-range collisions between like particles, Ar–Ar;
3) Coulomb collisions, e–e, e–Ar^+, Ar^+–Ar^+.

The collision algorithm for type (1) is derived from the linear Boltzmann equation, as described in Section II-A, that for type (2) is from the nonlinear Boltzmann equation, and that for type (3) is derived from the Landau–Fokker–Planck equation, which is a special form of the Boltzmann equation. The DSMC
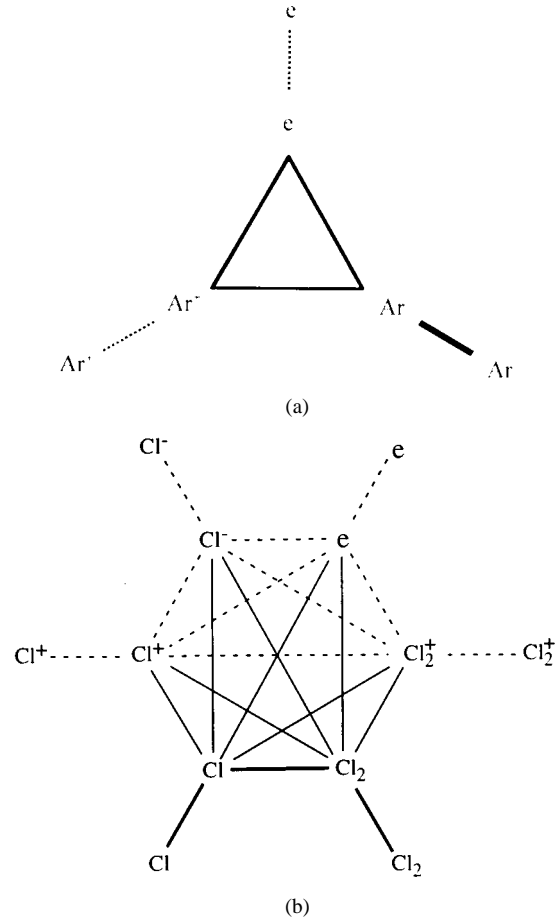

Fig. 1. Collisions in (a) argon plasma and (b) chlorine plasma.

method has been developed to simulate the collisions between neutral particles by rarefied gas dynamicists, whereas the PIC/MC method has been developed to simulate the collisions of charged particles by plasma physicists. Although the relation between the collision simulation method and the Boltzmann equation for a spatially homogeneous gas has been studied for the DSMC method, both the DSMC and PIC/MC methods are valid ways of solving the Boltzmann equation. If the E or B field is coupled with the particle motion, the method is called PIC/MC, and if not, the method is called DSMC. In the original DSMC [5], the time step Δt depended on the probable time to the next collision. However, it is held fixed in a recent DSMC [6], as has been done in PIC. Now, there is no other difference between the DSMC and PIC/MC methods.

Is it necessary to take all collisions in Fig. 1(a) into consideration? The answer depends on what plasma is being considered. Let n_e, n_+, and n_A be the number densities of e, Ar^+, and Ar, respectively. The collision rate between species i and j is proportional to $n_i n_j$ times the collision cross section, where i and j denote e, $+$, or A. A rough estimate is that if some $n_i n_j$ is much smaller than all other density products, we can disregard the i–j collisions. Let us consider some examples. The first is a capacitively coupled radiofrequency plasma with $n_e = n_+ = 10^{10}$ cm^{-3} and $n_A = 2 \times 10^{15}$ cm^{-3}. The ratio of $n_i n_j$ to n_A^2 is 5×10^{-6} for e–Ar, Ar^+–Ar, and 2.5×10^{-11} for Coulomb collisions. A large difference of order among density products suggests certain steps in the overall simulation procedure. First, gas

flow of Ar is calculated by considering only Ar–Ar collisions. Next, the plasma discharge in the flow of Ar is calculated by considering e–Ar and Ar^+–Ar collisions. Coulomb collisions can be disregarded in this case. This procedure is the first approximation. Because the flow of Ar are affected by the plasma through Ar^+–Ar collisions, this effect should be taken into consideration when obtaining the second approximation of the flow of Ar.

The second example is an inductively coupled plasma with $n_e = n_+ = 10^{12}$ cm^{-3} and $n_A = 2 \times 10^{14}$ cm^{-3}. The ratio of $n_i n_j$ to n_A^2 is 0.005 for e–Ar and Ar^+–Ar, and 2.5×10^{-5} for Coulomb collisions. In this case, the ratio of $n_+ n_A$ to n_A^2 is much larger than that for the capacitively coupled plasma, and hence, coupling of the gas flow with the plasma is stronger. Moreover, the Coulomb collisions should be taken into consideration in the plasma simulation. The overall simulation consists of the repetition of the following two stages.

1) Flow simulation of heavy particles Ar and Ar^+ from the calculation of all collisions among heavy particles.
2) Plasma simulation from the calculation of all types of collisions including electrons.

Species and collision pairs of chlorine plasma are depicted in Fig. 1(b). Chlorine plasma is employed in aluminum etching. Let us consider a typical inductively coupled plasma with $n(Cl_2) = n(Cl) = 2 \times 10^{14}$ cm^{-3}, $n(Cl_2^+) = n(Cl^-) = n(Cl^+) = 10^{12}$ cm^{-3}, and $n(e) = 10^{11}$ cm^{-3}. We consider the ratio of $n(i)n(j)$ to $[n(Cl_2)]^2$. The value of the ratio is 1 for a neutral–neutral collision, 5×10^{-3} for an ion–neutral collision, 5×10^{-4} for an electron–neutral collision, 2.5×10^{-5} for an ion–ion collision, 2.5×10^{-6} for an electron–ion collision, and 2.5×10^{-7} for an electron–electron collision. The flows of heavy particles Cl_2, Cl, Cl_2^+, Cl^+, Cl^- can be approximately treated separately from electrons. In plasma simulation, all types of collisions relevant to electrons should be considered. Note that Coulomb collisions are important in high-density plasmas.

A. Electron–Molecule Collision

Two methods of treating electron–molecule collisions are described.

1) Null-Collision Method: The probability that an electron collides with a molecule in time Δt is

$$P_T = \nu \Delta t \tag{28}$$

where ν is the collision rate given by

$$\nu = n_g v \sigma_T. \tag{29}$$

Here, n_g is the number density of gas, v is the speed of an electron, and σ_T is the total collision cross section; σ_T is a function of electron energy $\varepsilon (= mv^2/2)$ and is the sum of the integral collision cross sections for collisional events, such as elastic collision, vibrational excitation, electronic excitation, ionization, and dissociation. It is

$$\sigma_T = \sum_{k=1}^{K} \sigma_k \tag{30}$$

where σ_k is the integral cross section for the kth collisional event and K is the number of collisional events. Note that ν depends on time t because v is a function of time. Let us consider a collision in interval $(0, t+\Delta t)$. Let $Q(t+\Delta t)$ be the probability that the electron that started the motion at $t = 0$ spends time $t + \Delta t$ without collision. Then, we have

$$Q(t + \Delta t) = Q(t)[1 - \nu(t)\Delta t]$$

where $1 - \nu(t)\Delta t$ is the probability of no collision in $(t, t+\Delta t)$. In the limit of $\Delta t \to 0$, this equation takes the form $dQ/dt = -\nu(t)Q(t)$. Its solution is

$$Q(t) = \exp\left[-\int_0^t \nu(t)\,dt\right]. \tag{31}$$

Let T_c be the time of collision and $f_c(t)$ be its probability density function. Then, we have

$$Prob\{T_c < t_c\} = \int_0^{t_c} f_c(t)\,dt = 1 - Q(t_c). \tag{32}$$

Note that $Q(t_c)$ is equal to $Prob\{T_c > t_c\}$. The general rule for making a random sample t_c of the probability density function $f_c(t)$ is

$$\int_0^{t_c} f_c(t)\,dt\,[= 1 - Q(t_c)] = U \tag{33}$$

where U is a random number between 0 and 1. Once U is given, we could, in principle, obtain t_c from (31) and (33) and calculate a collision at $t = t_c$. Unless ν is constant, however, finding t_c by this method is time-consuming.

To overcome this difficulty, Skullerud [18] introduced a constant $\nu_{\max}$ that is larger than $\nu(t)$ at any t. If we replace ν by $\nu_{\max}$ in (31), from (33) we have

$$t_c' = -\nu_{\max}^{-1} \ln U \tag{34}$$

where t_c' denotes t_c in (33) and the equivalence of U and $1 - U$ is used. Let us consider the relation between the approximate value t_c' and the exact value t_c. The same random number U should be used in determining t_c and t_c' from (33); $Q(t_c)$ for the rate $\nu(t)$ and $Q(t_c')$ for the rate $\nu_{\max}$ are equal, and hence

$$\int_0^{t_c} \nu(t)\,dt = \int_0^{t_c'} \nu_{\max}\,dt.$$

Because $\nu_{\max} > \nu(t)$, we have $t_c' < t_c$; the collision time t_c' is smaller than is the exact value t_c. When a collision is considered at $t = t_c'$, the following correction is necessary. We write the probabilities $Prob\{T_c < t_c'\}$ for the rates ν and $\nu_{\max}$, respectively, as

$$P_c = 1 - \exp\left[-\int_0^{t_c'} \nu(t)\,dt\right]$$
$$(P_c)_{\max} = 1 - \exp(-\nu_{\max} t_c'). \tag{35}$$

Note that $P_c < (P_c)_{\max}$. The collision at $t = t_c'$ is regarded as a real collision with a probability of $P_c/(P_c)_{\max}$ and as a null collision with a probability of $1 - P_c/(P_c)_{\max}$. In the latter case, no change in electron velocity occurs . This method is computationally efficient because of no need of finding t_c from
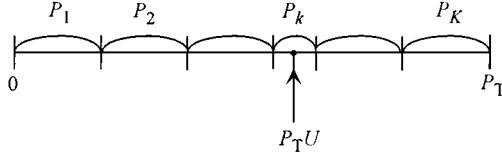
Fig. 2.   Usual method to sample a collisional event.

(33). If t'_c is sufficiently small, $\nu(t)$ in (35) can be approximated by a quadratic equation and the integral becomes

$$\int_0^{t'_c} \nu(t)\,dt = \frac{t'_c}{6}\left[\nu(0) + 4\nu(t'_c/2) + \nu(t'_c)\right]. \quad (36)$$

This equation can be used in evaluating P_c of (35).

A collisional event at time t'_c is chosen as follows. The probability of occurrence of a kth event in interval $(0, t'_c)$ is

$$P_k = 1 - \exp\left[-\int_0^{t'_c} \nu_k(t)\,dt\right]. \quad (37)$$

The sum of P_k's is

$$P_T = \sum_{k=1}^{K} P_k.$$

The event k should be sampled with a probability of P_k/P_T. Sampling is done as is shown in Fig. 2; if the position $P_T U$ is in the interval of P_k, the kth collisional event occurs, where U is a random number between 0 and 1.

The null collision method is computationally efficient. The method is useful in calculating swarm parameters in a uniform electric field. In a general PIC/MC simulation, the electromagnetic field should be calculated at given time points with equal spacing. In such a case, the null-collision method is inconvenient because the collision time is different from electron to electron. In the following method, this inconvenience is alleviated by allowing more time for computation.

2) Constant Time-Step Method: Let us consider time interval $(t, t + \Delta t)$. The position and velocity of an electron at time $t + \Delta t$ are calculated from the equation of motion by use of the velocity and position at time t. The collision in $(t, t + \Delta t)$ can be calculated separately from the calculation of motion if the chosen Δt is much smaller than is the mean free time. This principle of decoupling stems from the operator splitting described in Section II-A. There is no need to consider the occurrence of a collision between t and $t + \Delta t$; it is sufficient to consider that a possible collision occurs at $t + \Delta t$ with the velocity at the end of the collisionless motion.

Equation (28) can be written as

$$P_T = \sum_{k=1}^{K} P_k \quad (38)$$

where

$$P_k = n_g v \sigma_k \Delta t. \quad (39)$$

Here, v is the electron speed. Nanbu [19] proposed a simple method to simultaneously determine whether an electron col-
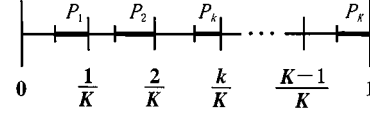

Fig. 3.   Nanbu's method to sample a collisional event.

lides and which collisional event occurs in the case of collision. He wrote (38) as

$$1 = P_T + (1 - P_T) = \sum_{k=1}^{K}\left[P_k + \left(\frac{1}{K} - P_k\right)\right]. \quad (40)$$

This equation is depicted in Fig. 3. The unit length is divided into K equal intervals. Each interval is divided into two. Let us examine the kth interval. The length of its left part is $1/K - P_k$ and that of its right part is P_k. The sum of the right parts is equal to P_T, and the sum of the left parts is equal to $1 - P_T$. Note that $P_1, P_2, \ldots, P_K$ are the probability of occurrence of collisional events $1, 2, \ldots, K$. Let us choose a random number and call it U. If this U is in one of the right parts, say, the right part of the kth interval, an electron collides and the kth collisional event occurs. Clearly, if U is in one of the left parts, the electron does not collide. The integral part of $1 + UK$ is the number of the interval to which U belongs. If k is that interval, we have only to calculate P_k to determine whether the position of U is in the left or right part of the kth interval. Note that only one random number is used in this procedure.

3) Postcollision Velocity of Electron: Let $\boldsymbol{g} = \boldsymbol{v} - \boldsymbol{V}$ be the relative velocity between an electron with velocity $\boldsymbol{v}$ and a molecule with velocity $\boldsymbol{V}$. The magnitude g can be replaced by v because $v \gg V$. The deflection angle of the relative velocity χ is determined from the differential collision cross section $\sigma(v, \chi)$. The integral cross section $\sigma_k(v)$ in (39) is defined by

$$\sigma_k(v) = \int_0^{2\pi} d\psi \int_0^{\pi} \sigma(v, \chi)\sin\chi\,d\chi \quad (41)$$

where

$\sin\chi\,d\chi\,d\psi$ solid angle into which the postcollision velocity of the electron $\boldsymbol{v}'$ is directed;
χ polar angle;
ψ azimuthal angle.

The probability that $\boldsymbol{v}'$ is in the solid angle $\sin\chi\,d\chi\,d\psi$ is $\sigma\sin\chi\,d\chi\,d\psi/\sigma_k$, which is the product of $(2\pi)^{-1}\,d\psi$ and $2\pi(\sigma/\sigma_k)\sin\chi\,d\chi$. The coefficient $(2\pi)^{-1}$ of $d\psi$ is the probability density function of ψ; a random sample of ψ is

$$\psi = 2\pi U. \quad (42)$$

The coefficient $2\pi(\sigma/\sigma_k)\sin\chi$ of $d\chi$ is the probability density function of the deflection angle χ; a random sample χ is calculated using

$$\frac{2\pi}{\sigma_k(v)}\int_0^{\chi} \sigma(v, \chi')\sin\chi'\,d\chi' = U. \quad (43)$$

We see from (43) that χ is a function of v and U.

Published data on the differential cross sections are far from sufficient for many types of collisions. If there is no data, the cross section $\sigma(v, \chi)$ is assumed not to depend on χ. Equation (41) then gives $\sigma_k = 4\pi\sigma$. The probability $\sigma\sin\chi\,d\chi\,d\psi/\sigma_k$ becomes $\sin\chi\,d\chi\,d\psi/4\pi$. This means that the postcollision ve-

locity $\boldsymbol{v}'$ takes a random direction. The scattering with this property is termed isotropic. Here, all scatterings are assumed to be isotropic. A realistic scattering is considered in Sections III-A4 and III-A5.

First, we consider elastic and exciting collisions. Ionizing collisions are then treated. Let m and M be the masses of an electron and a molecule, respectively. The conservation of momentum and energy are

$$m\boldsymbol{v}' + M\boldsymbol{V}' = m\boldsymbol{v} + M\boldsymbol{V} \tag{44a}$$

$$\tfrac{1}{2}\mu(\boldsymbol{v}' - \boldsymbol{V}')^2 + E = \tfrac{1}{2}\mu(\boldsymbol{v} - \boldsymbol{V})^2 \tag{44b}$$

where
the primes denote the postcollision velocities;
$\mu[= mM/(m+M)]$ reduced mass;
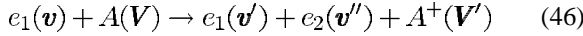E threshold energy of excitation.
We set $E = 0$ for elastic collision. From (44b), we thus have

$$\boldsymbol{v}' - \boldsymbol{V}' = \left[(\boldsymbol{v} - \boldsymbol{V})^2 - \frac{2E}{\mu}\right]^{1/2} \boldsymbol{R} \tag{45}$$

where $\boldsymbol{R}$ is the unit vector with a random direction. The postcollision velocities $\boldsymbol{v}'$ and $\boldsymbol{V}'$ can be determined from (44a) and (45).

Next, let us consider an e–A ionizing collision, where A denotes a molecule. The collision is represented as

$$e_1(\boldsymbol{v}) + A(\boldsymbol{V}) \rightarrow e_1(\boldsymbol{v}') + e_2(\boldsymbol{v}'') + A^+(\boldsymbol{V}') \tag{46}$$

where A^+ denotes an ion and the symbols in the parentheses denote the velocities. The conservation equations are

$$m\tilde{\boldsymbol{v}}' + m\tilde{\boldsymbol{v}}'' + (M - m)\tilde{\boldsymbol{V}}' = 0 \tag{47}$$

$$\tfrac{1}{2}m\tilde{v}'^2 + \tfrac{1}{2}m\tilde{v}''^2 + \tfrac{1}{2}(M - m)\tilde{V}'^2 + E = \tfrac{1}{2}\mu(\boldsymbol{v} - \boldsymbol{V})^2 \tag{48}$$

where E is the threshold energy of ionization and $(\tilde{})$ denotes the velocity from which the center-of-mass velocity $\boldsymbol{W}$ is subtracted

$$\boldsymbol{W} = \frac{m\boldsymbol{v} + M\boldsymbol{V}}{m + M}. \tag{49}$$

From (47), we have

$$\tilde{\boldsymbol{V}}' = -(m/M)(\tilde{\boldsymbol{v}}' + \tilde{\boldsymbol{v}}'') \tag{50}$$

where $m \ll M$ is used. Substitution of (50) into (48) shows that the third term in the left-hand side is negligibly small compared with the first two terms. After omission of the third term, (48) takes the form

$$\tfrac{1}{2}m\tilde{v}'^2 + \tfrac{1}{2}m\tilde{v}''^2 = \tfrac{1}{2}\mu(\boldsymbol{v} - \boldsymbol{V})^2 - E(\equiv \Delta E). \tag{51}$$

The right-hand side is known and denotes the excess energy ΔE after ionization. In the case when there is no published work on the division of ΔE into two electrons, ΔE is divided randomly into two as

$$\tfrac{1}{2}m\tilde{v}'^2 = U\Delta E \tag{52a}$$

$$\tfrac{1}{2}m\tilde{v}''^2 = (1 - U)\Delta E \tag{52b}$$

where the two U's denote the same random number. Assuming that $\tilde{\boldsymbol{v}}'$ and $\tilde{\boldsymbol{v}}''$ are isotropic, we have

$$\tilde{\boldsymbol{v}}' = \tilde{v}'\boldsymbol{R} \tag{53a}$$

$$\tilde{\boldsymbol{v}}'' = \tilde{v}''\boldsymbol{R}' \tag{53b}$$

where $\tilde{v}'$ and $\tilde{v}''$ are obtained from (52a) and (52b), and $\boldsymbol{R}$ and $\boldsymbol{R}'$ are different unit vectors with a random direction. Once $\tilde{\boldsymbol{v}}'$
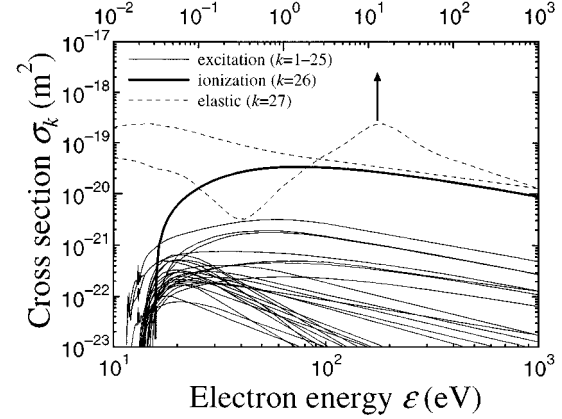

Fig. 4. Electron impact collision cross section of argon.

and $\tilde{\boldsymbol{v}}''$ are obtained, $\tilde{\boldsymbol{V}}'$ is given by (50). The velocities in the laboratory frame-of-reference are obtained by adding $\boldsymbol{W}$ to $\tilde{\boldsymbol{v}}'$, $\tilde{\boldsymbol{v}}''$, and $\tilde{\boldsymbol{V}}'$.

4) Electron–Argon Atom Collision: For an e–Ar collision, there is a detailed set of collision data. Fig. 4 shows a set of integral cross sections given by Kosaki and Hayashi [20]; the 27 collisional events considered consist of an elastic collision, an ionizing collision, and 25 exciting collisions. The ionizing cross section of Kosaki and Hayashi is replaced by 0.9 times Peterson and Allen's cross section [21]. The latter agrees well with the table recommended by Kosaki and Hayashi. The differential cross section σ is modeled for all collisional events by Surendra *et al.* [22] as

$$\sigma(v, \chi) = \sigma_k g(\chi)$$

where σ_k denotes the integral cross section for the kth event and $g(\chi)$ is given by

$$g(\chi) = \frac{\varepsilon}{4\pi[1 + \varepsilon\sin^2(\chi/2)]\ln(1 + \varepsilon)} \tag{54}$$

$\varepsilon(= mv^2/2)$ being the electron energy in units of eV. As $\varepsilon \to 0$, $g(\chi) \to 1/4\pi$, and hence, scattering is isotropic. For large ε, the function $g(\chi)$ takes a form of forward scattering. A random sample of $\cos\chi$ can be easily obtained. It is

$$\cos\chi = \frac{1}{\varepsilon}\left[\varepsilon + 2 - 2(1 + \varepsilon)^U\right] \tag{55}$$

where U is a random number between 0 and 1. A random sample of azimuthal angle ψ is in (42). The postcollision velocities for an elastic collision are given by [23]

$$\boldsymbol{v}' = \boldsymbol{v} - \frac{M}{M + m}[\boldsymbol{g}(1 - \cos\chi) + \boldsymbol{h}\sin\chi] \tag{56a}$$

$$\boldsymbol{V}' = \boldsymbol{V} + \frac{m}{M + m}[\boldsymbol{g}(1 - \cos\chi) + \boldsymbol{h}\sin\chi] \tag{56b}$$

where $\boldsymbol{g} = \boldsymbol{v} - \boldsymbol{V}$, $\boldsymbol{v}$ and $\boldsymbol{V}$ are the precollision velocities of e and Ar, and the Cartesian components of $\boldsymbol{h}$ are

$$h_x = g_\perp\cos\psi$$
$$h_y = -(g_x g_y\cos\psi + gg_z\sin\psi)/g_\perp$$
$$h_z = -(g_x g_z\cos\psi - gg_y\sin\psi)/g_\perp$$

where $g_\perp = (g_y^2 + g_z^2)^{1/2}$. Equations (56a) and (56b) hold for any m/M; these equations can be somewhat simplified by use of $M + m \simeq M$ and $\boldsymbol{g} \simeq \boldsymbol{v}$.

Next, let us consider electronic excitation in an e–Ar collision [22]. Because $V' \ll v'$, $V \ll v$, and $\mu \simeq m$ hold in (44b), we have

$$v' = \left(v^2 - \frac{2E}{m} \right)^{1/2}.$$

Let us define the velocity $\tilde{\boldsymbol{v}}$ with magnitude v' and direction $\boldsymbol{v}/v$ by

$$\tilde{\boldsymbol{v}} = \boldsymbol{v} \left(1 - \frac{E}{\varepsilon} \right)^{1/2} \tag{57}$$

where $\varepsilon (= mv^2/2)$ is the energy before collision. An exciting e–Ar collision is treated as if it were an elastic collision with precollision velocities $\tilde{\boldsymbol{v}}$ and $\boldsymbol{V}$; the velocities $\boldsymbol{v}'$ and $\boldsymbol{V}'$ after an exciting collision are given by (56a) and (56b) in which all $\boldsymbol{v}$'s are replaced by $\tilde{\boldsymbol{v}}$. The validity of this treatment is soon discussed.

Lastly, let us consider the ionizing collision of (46). Let us call electron e_1 parent and electron e_2 progeny. Equation (51) can be approximated as

$$\tfrac{1}{2}mv^2 - \tfrac{1}{2}mv'^2 = E + \varepsilon_p (\equiv \Delta\varepsilon) \tag{58}$$

where $\Delta\varepsilon$ is the energy loss of the parent and $\varepsilon_p (= mv''^2/2)$ is the energy of the progeny. In deriving (58) v', $v'' \gg W$ is assumed in addition to $v \gg V$ and $m \ll M$. Note that the condition v', $v'' \gg W$ requires v', $v'' \gg (m/M)v$ and v', $v'' \gg V$. It is required that the progeny's energy ε_p be less than is the postcollision energy $mv'^2/2$ of the parent [21]; i.e., we have $0 < \varepsilon_p < (\varepsilon - E)/2$ from (58), where $\varepsilon = mv^2/2$. The probability density function $g(\varepsilon_p)$ for ε_p is [21]

$$g(\varepsilon_p) = \frac{a}{(\varepsilon_p - \varepsilon_0)^2 + a^2} \left(\tan^{-1} \frac{\varepsilon_1}{a} + \tan^{-1} \frac{\varepsilon_0}{a} \right)^{-1}$$
$$\varepsilon_0 = 2 - \frac{100}{\varepsilon + 10}$$
$$\varepsilon_1 = \frac{\varepsilon - E}{2} - \varepsilon_0$$
$$a = 10.3.$$

The units of ε_p, ε_0, and ε_1 are electronvolts. A random sample of ε_p is given by

$$\varepsilon_p = \varepsilon_0 + a \tan\left[U\left(\tan^{-1} \frac{\varepsilon_1}{a} + \tan^{-1} \frac{\varepsilon_0}{a} \right) - \tan^{-1} \frac{\varepsilon_0}{a} \right]$$

where U is a random number between 0 and 1. Once ε_p is sampled, v' from (58) is

$$v' = \left[v^2 - \frac{2(E + \varepsilon_p)}{m} \right]^{1/2}.$$

Define $\tilde{\boldsymbol{v}} = v'(\boldsymbol{v}/v)$ as before

$$\tilde{\boldsymbol{v}} = \boldsymbol{v}\left(1 - \frac{E + \varepsilon_p}{\varepsilon} \right)^{1/2}.$$

The postcollision velocity $\boldsymbol{v}'$ of the parent is obtained by replacing $\boldsymbol{v}$ by $\tilde{\boldsymbol{v}}$ in (56a). The precollision velocity cannot be imagined for the progeny. However, the precollision velocity of $\tilde{\boldsymbol{v}}_p = (\boldsymbol{v}/v)\sqrt{2\varepsilon_p/m}$ is assumed, and the postcollision velocity $\boldsymbol{v}'_p$ is obtained from (56a) by replacing $\boldsymbol{v}$ by $\tilde{\boldsymbol{v}}_p$ and $\boldsymbol{v}'$ by $\boldsymbol{v}'_p$.
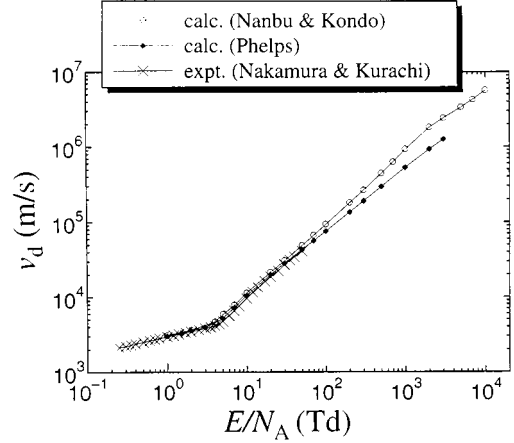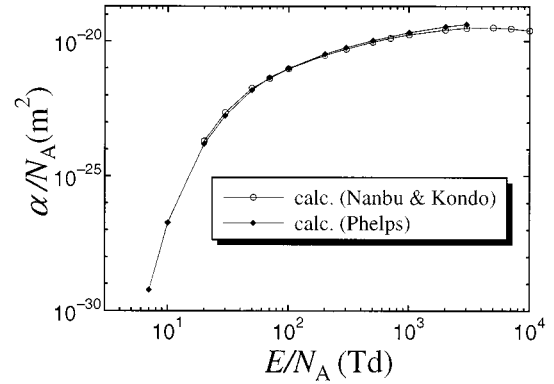

Fig. 5.   Electron drift velocity in argon.

Fig. 6.   Electron impact ionization coefficient for argon.

We have seen that several assumptions are employed in determining the velocity of an electron after electronic excitation or ionization. The validity of the collision model described in this section should be examined by calculating swarm parameters, such as electron drift velocity. Nanbu and Kondo [16] showed that the calculated drift velocity v_d agrees very well with the measured data of Nakamura and Kurachi [24]. This is shown in Fig. 5, where the data of Phelps [25] is added. In Fig. 5, E is the electric field and N_A is the argon number density. Fig. 6 shows that the ionization coefficient α obtained by use of the above model also agrees well with Phelps' data.

5) Electron–Cl₂ and Electron–Cl Collisions: Molecular chlorine is used in plasma etching where Cl atoms produced in a gas discharge etch an aluminum or silicon surface. A detailed set of cross sections has been reported by Christophorou and Olthoff [26] and Morgan [27]. In particle simulation, we need a differential cross section with a simple form. Here, we propose models of such a differential cross section for elastic scattering. First, let us consider an e–Cl₂ collision. Rescigno [28] reported the total elastic scattering cross section $\sigma_{el}(\varepsilon)$ and momentum transfer cross section $\sigma_m(\varepsilon)$ for $\varepsilon < 30$ eV. See Fig. 7. If scattering is isotropic, the definition of $\sigma_m(\varepsilon)$ yields $\sigma_m(\varepsilon) = \sigma_{el}(\varepsilon)$ for any ε. There is a clear difference between the two cross sections: Scattering is not isotropic. Our model for the differential cross section $\sigma(v, \chi)$ is

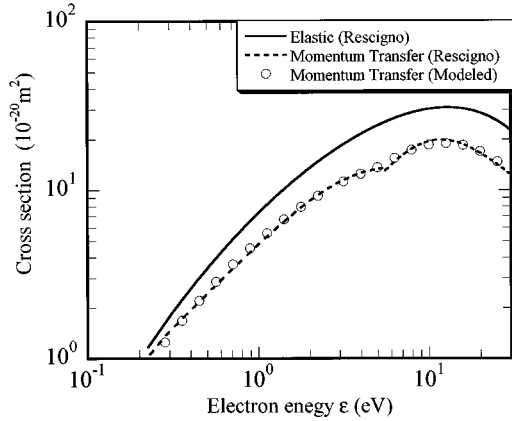$$\sigma(v, \chi) = \sigma_{el}(\varepsilon) f(\chi, \varepsilon)$$

Fig. 7.   e–Cl_2 momentum transfer cross sections. The circles represent the momentum transfer cross section resulting from the present model of differential cross section, and the dashed line represents Rescigno's data.
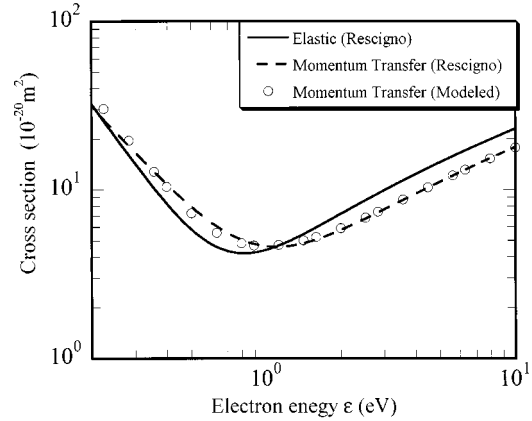

Fig. 8.   e–Cl momentum transfer cross sections. The circles represent the cross section resulting from the present model of differential cross section, and the dashed lines represents Rescigno's data.

where

$$f(\chi, \varepsilon) = A \exp[-\alpha \sin^2(\chi/2)]$$

and $A[= \alpha/4\pi(1 - e^{-\alpha})]$ is the normalization constant. We set $\alpha = 2\varepsilon^{1/4}$ for $\varepsilon < 5.5$ eV and $\alpha = 0.5\sqrt{\varepsilon} + 10/\varepsilon$ for 5.5 eV $< \varepsilon < 30$ eV. The form of $f(\chi, \varepsilon)$ is chosen based on the measurements of Gote and Ehrhardt [29] for $\varepsilon = 5$ eV. The parameter α is chosen in such a way that $\sigma_m(\varepsilon)$ resulting from the present model of $\sigma(v, \chi)$ agrees with Rescigno's $\sigma_m(\varepsilon)$. Fig. 7 shows that the two σ_m's agree well. A random sample of the scattering angle χ is given analytically

$$\cos \chi = 1 + \frac{2}{\alpha} \ln[(1 - e^{-\alpha})U + e^{-\alpha}].$$

Similarly, we made a model of $\sigma(v, \chi)$ for electron–Cl collision based on Rescigno's unpublished data [27] on $\sigma_{el}(\varepsilon)$ and $\sigma_m(\varepsilon)$: $\sigma_{el}(\varepsilon) = -6.192 + 9.226\sqrt{\varepsilon} + 1.376\varepsilon^{-2}$ for 0.2 eV $< \varepsilon < 10.0$ eV. The form of function $f(\chi, \varepsilon)$ is chosen based on Rescigno's results of calculation [27]. Our model is

$$f(\chi, \varepsilon) = A e^{-\alpha\chi} + B e^{-\beta(\pi - \chi)}$$

where $\alpha = 0.6$, $\beta = 0.8/\varepsilon$, $B = e^{-2\varepsilon}$, and

$$A = \frac{\alpha^2 + 1}{2\pi(e^{-\pi\alpha} + 1)} \left[1 - \frac{2\pi B}{\beta^2 + 1}(e^{-\pi\beta} + 1)\right].$$

The momentum transfer cross section resulting from the present model is compared in Fig. 8 with Rescigno's $\sigma_m(\varepsilon)$. Agreement of the two σ_m's is good. A random sample of χ of the probability density function $2\pi f(\chi, \varepsilon) \sin \chi$ must be obtained by use of the acceptance–rejection method [5].

B. Ion–Molecule Collision

1) Hard-Sphere Interaction: Interaction between an ion and a molecule is short range. The algorithm for an ion–molecule collision is, therefore, essentially the same as that for a molecule–molecule collision. The only difference is the charge-exchange in ion–molecule collision. Let us consider the elastic collisions without charge-exchange

$$A^+(\boldsymbol{v}_A) + B(\boldsymbol{v}_B) \rightarrow A^+(\boldsymbol{v}'_A) + B(\boldsymbol{v}'_B) \qquad (59)$$

and with charge-exchange

$$A^+(\boldsymbol{v}_A) + B(\boldsymbol{v}_B) \rightarrow A(\boldsymbol{v}'_A) + B^+(\boldsymbol{v}'_B). \qquad (60)$$

If gas B is at rest and in equilibrium at temperature T_B, the probability that ion A^+ elastically collides with some molecule B is

$$P_c = n_B \overline{g\sigma_T(g)} \Delta t \qquad (61)$$

where n_B is the number density of gas B, $g = |\boldsymbol{v}_A - \boldsymbol{v}_B|$ is the relative velocity, and the average is taken over the Maxwellian distribution of $\boldsymbol{v}_B$. Note that $\sigma_T(g)$ is the sum of the collision cross sections with and without charge-exchange. If the ion–molecule interaction is treated by use of the hard-sphere model, σ_T is the constant given by πd_{AB}^2, where $d_{AB} = (d_A + d_B)/2$, and d_A and d_B are the radii of the ion and the molecule, respectively. In this case, we have $P_c = n_B \overline{g} \sigma_T \Delta t$, where [31]

$$\overline{g} = \sqrt{2R_B T_B} \left[\left(\eta_A + \frac{1}{2\eta_A}\right) \mathrm{erf}\eta_A + \frac{1}{\sqrt{\pi}} \exp\left(-\eta_A^2\right)\right].$$

Here, $R_B = k/m_B$, $\eta_A = v_A/\sqrt{2R_B T_B}$, k is the Boltzmann constant, and m_B is the mass of molecule B.

If gas B is in nonequilibrium, we use the DSMC method; the average in (61) is for all simulated molecules in a cell.

$$P_c = \frac{n_B}{N_B} \sum_{j=1}^{N_B} g_j \sigma_T(g_j) \Delta t \qquad (62)$$

where N_B is the number of simulated molecules whose velocities are $\boldsymbol{v}_{B1}, \boldsymbol{v}_{B2}, \ldots$, and $g_j = |\boldsymbol{v}_A - \boldsymbol{v}_{Bj}|$. The jth term $N_B^{-1} n_B g_j \sigma_T(g_j) \Delta t$ in (62) represents the probability that an ion collides with a molecule with velocity $\boldsymbol{v}_{Bj}$; a collision partner of the ion should be chosen with a probability proportional to $g_j \sigma_T(g_j)$.

If A^+–B collision is treated by the hard-sphere model, the scattering is isotropic. Then, the postcollision velocities for (59) are

$$\boldsymbol{v}'_A = \frac{1}{m_A + m_B} (m_A \boldsymbol{v}_A + m_B \boldsymbol{v}_B + m_B |\boldsymbol{v}_A - \boldsymbol{v}_B| \boldsymbol{R})$$

$$(63a)$$

$$\boldsymbol{v}'_B = \frac{1}{m_A + m_B} (m_A \boldsymbol{v}_A + m_B \boldsymbol{v}_B - m_A |\boldsymbol{v}_A - \boldsymbol{v}_B| \boldsymbol{R})$$

$$(63b)$$

where the two $\boldsymbol{R}$'s are the same unit vector with a random direction. The same equations hold for (60). However, the postcollision velocity of the ion is $\boldsymbol{v}'_B$ for (60). In case of $m_A = m_B$ as in the case of an Ar^+–Ar or a Cl_2^+–Cl_2 collision, the ion velocity is

$$\tfrac{1}{2}(\boldsymbol{v}_A + \boldsymbol{v}_B \pm |\boldsymbol{v}_A - \boldsymbol{v}_B|\boldsymbol{R})$$

where plus is for (59) and minus is for (60). Because $+\boldsymbol{R}$ and $-\boldsymbol{R}$ have the same probabilistic character, the ion velocity is essentially the same despite whether a charge-exchange occurs. This unfavorable property limits utility of the hard-sphere model for $m_A = m_B$. In dc or rf discharges, an ion which gained a high kinetic energy in a sheath is changed into an ion with thermal energy after a charge–exchange collision. This effect cannot be taken into consideration if the hard-sphere model is used as it stands.

A simple correction is to treat the charge-exchange by use of the identity switch model. In this model, the charge of an ion is transferred to a molecule without the velocity of either being changed. We thus have $\boldsymbol{v}'_A = \boldsymbol{v}_A$ and $\boldsymbol{v}'_B = \boldsymbol{v}_B$ for (60). The ion velocity relative to molecular velocity is changed from $\boldsymbol{v}_A - \boldsymbol{v}_B$ to $-(\boldsymbol{v}_A - \boldsymbol{v}_B)$, and hence, the deflection angle of the ion is π. The charge-exchange in a sheath can be taken into consideration by using this π-scattering model. A combination of a half hard-sphere elastic collision and a half π-scattering charge-exchange may be a reasonable approximation because the charge-exchange probability is 1/2 [32]. See (66a). The validity of this model was examined by calculating drift velocity v_d and transverse diffusion coefficient D_T [33]. The molecular diameter d_B was set to be equal to the viscosity diameter [34]. It was found that if the collision cross section πd_{AB}^2 is chosen to be equal to $2\pi d_B^2$, the obtained values of v_d and $D_T/(v_d/E)$ show reasonable agreement with the existing data [35], [36] for He^+ in He, Ne^+ in Ne, Ar^+ in Ar, and Kr^+ in Kr. The drift velocity of Ar^+ in Ar resulting from the present model is compared in Fig. 9 with the measured data, where N_A denotes the number density of Ar. The agreement is reasonable.

2) Induced Dipole Interaction: Nanbu and Kitatani [37] proposed a more accurate model for He^+–He, Ne^+–Ne, Ar^+–Ar, and Kr^+–Kr collisions. They determined a free parameter in their model by use of measured ion drift velocities. The ion–molecule interaction was expressed by the Langevin–Hassé model; the polarization potential, $-a/r^4$, with a hard core, where a is a constant and r is the distance between the ion and the molecule. Although the original Langevin–Hassé model is valid only for small relative collision energy, Nanbu and Kitatani's version holds from small energy, say, 10^{-2} eV to high energy, such as 10^3 eV. The free parameter in Nanbu and Kitatani's model is the limiting impact parameter below which charge-exchange is assumed possible. We now describe the outline of this model.

Let us consider the collision of a single-charged ion A with molecule B. The collision probability of the ion in time Δt is given by (61). It takes the form

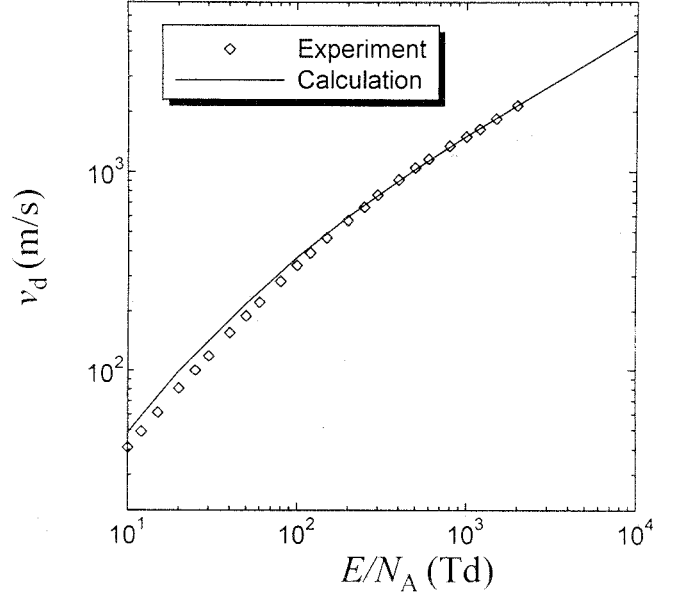$$P_c = n_B \left(\frac{8a}{\mu}\right)^{1/2} \pi \beta_\infty^2 \Delta t \qquad (64)$$

Fig. 9. Drift velocity of Ar^+ in Ar. The solid line represents the results obtained by use of the hard sphere plus π-scattering model.

for the polarization potential, where $a = \alpha_d e^2/[2(4\pi\epsilon_0)^2]$, $\alpha_d/(4\pi\epsilon_0)$ is the polarizability of molecule, e.g., $1.642\ \overset{\circ}{A}^3$ for Ar, e is the electronic charge, ϵ_0 is the dielectric constant of vacuum, $\mu = m_A m_B/(m_A + m_B)$ is the reduced mass, and $\beta_\infty (=9)$ is the cutoff of the dimensionless impact parameter

$$\beta = b\left(\frac{\varepsilon}{4a}\right)^{1/4}.$$

Here, $\varepsilon = \mu g^2/2$ is the relative collision energy, $g = |\boldsymbol{v}_A - \boldsymbol{v}_B|$ is the relative speed, and b is the impact parameter. Note that P_c of (64) is constant. This means that any molecule B is equally probable as a collision partner of ion A; a partner molecule can be randomly sampled from a set of molecules in a cell. Let $\boldsymbol{v}_B$ be the velocity of a sampled partner. First, we make a random sample of β. Because the probability density function for β is $2\beta/\beta_\infty^2$, it is given by

$$\beta = \beta_\infty \sqrt{U} \qquad (65)$$

where U is a random number between 0 and 1. In case of $\beta < 1$, an ion is reflected on the hard-core potential and the postcollision velocities are given by (63a) and (63b). The charge-exchange for $\beta < 1$ occurs with probability 1/2; if a charge-exchange occurs, $\boldsymbol{v}'_B$ is the ion velocity.

Next, let us consider the case of $\beta > 1$. The charge-exchange probability P_{ex} is given by

$$P_{ex} = \tfrac{1}{2} \quad \text{for } \beta < \beta_{ex}(\varepsilon) \qquad (66a)$$
$$P_{ex} = 0 \quad \text{for } \beta > \beta_{ex}(\varepsilon) \qquad (66b)$$

where

$$\beta_{ex} = C\varepsilon^{1/4}. \qquad (67)$$

The constant C $[=b_{ex}/(4a)^{1/4}]$ is determined in such a way that the drift velocity resulting from this charge-exchange model agrees with the experimental data. The value C is 2.6 for Ar^+–Ar, Ne^+–Ne, and He^+–He collisions and 2.5 for a

Kr^+–Kr collision. The units of ε are electronvolts for these values of C. If $\beta_{ex}(\varepsilon) < 1$, set $\beta_{ex}(\varepsilon) = 1$.

The deflection angle of the relative velocity $\boldsymbol{g}\,(=\boldsymbol{v}_A - \boldsymbol{v}_B)$ is a function of $\beta\,(=\beta_\infty\sqrt{U})$. It is

$$\chi(\beta) = \pi - \frac{2^{3/2}\beta}{\xi_1}K(\zeta)$$

where $\zeta = \xi_0/\xi_1$, $\xi_0 = [\beta^2 - (\beta^4-1)^{1/2}]^{1/2}$, $\xi_1 = [\beta^2 + (\beta^4 - 1)^{1/2}]^{1/2}$, and $K(\zeta)$ is the complete elliptic integral of the first kind

$$K(\zeta) = \int_0^{\pi/2}\frac{d\theta}{(1 - \zeta^2\sin^2\theta)^{1/2}}.$$

Because $\chi < 0$, let us define the polar angle χ' of $\boldsymbol{g}$ as $\chi' = |\chi|$ for $-\pi < \chi < 0$, $\chi' = 2\pi - |\chi|$ for $-2\pi < \chi < -\pi$, and so on. The azimuthal angle ψ of a collision plane is given by $\psi = 2\pi U$. The postcollision velocities of ion A and molecule B without charge-exchange are

$$\boldsymbol{v}'_A = \boldsymbol{v}_A - \frac{m_B}{m_A + m_B}[\boldsymbol{g}(1 - \cos\chi) + \boldsymbol{h}|\sin\chi|]$$

$$\boldsymbol{v}'_B = \boldsymbol{v}_B + \frac{m_A}{m_A + m_B}[\boldsymbol{g}(1 - \cos\chi) + \boldsymbol{h}|\sin\chi|]$$

where

$$h_x = g_\perp\cos\psi$$
$$h_y = (g_xg_y\cos\psi - gg_z\sin\psi)/g_\perp$$
$$h_z = (g_xg_z\cos\psi + gg_y\sin\psi)/g_\perp$$

$g_\perp = (g_y^2 + g_z^2)^{1/2}$, and $\cos\chi' = \cos\chi$ and $\sin\chi' = |\sin\chi|$ are used. When a charge-exchange occurs, $\boldsymbol{v}'_B$ is the ion velocity and $\boldsymbol{v}'_A$ is the molecular velocity. The constant C for gases other than inert gases can be determined if the data of drift velocity are given.

Fig. 10 shows the drift velocity resulting from Nanbu and Kitatani's model. The dashed line represents Mason and Viehland's moment theory. The deviation from the moment theory for $E/N_A > 10^5$ is due to the violation of condition $\beta_{ex}(\varepsilon) < \beta_\infty$. If the chosen β_∞ is larger than 9 (say, 15), the deviation disappears.

C. Molecule–Molecule Collision

1) Variable Hard-Sphere Model: The most accurate Lennard–Jones potential is not suited for the DSMC method because collision calculation is time-consuming. The simple inverse-power potential $V(r) = a/r^\alpha$ is sufficiently accurate and very efficient for collision calculation. The differential cross section σ for the inverse-power potential takes the form

$$\sigma = Ag^{-4/\alpha}\tag{68}$$

where g is the relative speed and A is a function of the deflection angle χ. If A is independent of χ, the probability $\sigma\,d\Omega/\sigma_T$ that the postcollision relative velocity is directed into the solid angle $d\Omega$ becomes $d\Omega/4\pi$; the scattering is isotropic. In this case, the postcollision velocities are simply given by (63a) and (63b). The variable hard-sphere (VHS) model was proposed by Bird [6] with the intention of avoiding the divergence of the total collision cross section and using isotropic scattering for the inverse-power potential. Bird's idea is as follows. Hereafter, the coefficient A is regarded as being constant. First, we consider
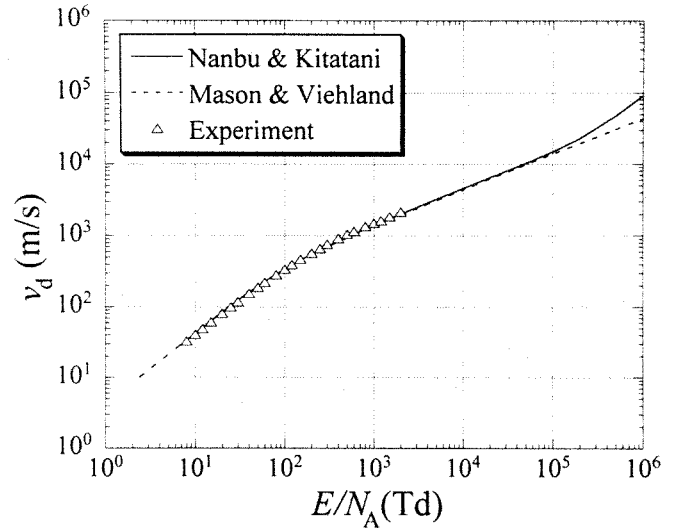

Fig. 10. Drift velocity of Ar^+ in Ar. The solid line represents the results obtained by use of Nanbu and Kitatani's collision model, and the dashed line represents Mason and Viehland's moment theory.

a simple gas. The Chapman–Enskog viscosity for $\sigma = Ag^{-4/\alpha}$ is given by [38]

$$\mu = \frac{15}{32\Gamma(4 - 2/\alpha)A}\left(\frac{mkT}{\pi}\right)^{1/2}\left(\frac{4kT}{m}\right)^{2/\alpha}\tag{69}$$

where

μ viscosity at temperature T;
m mass of a molecule;
k Boltzmann constant.

We see from (69) that $\mu \propto T^\eta$, where $\eta = (\alpha + 4)/2\alpha$. The index η is known for many gases; once a gas is specified, α is known. Using μ at some temperature T, we can determine the constant A by (69). Note that the value of A thus determined does not depend on the temperature at which μ is given.

The mean free path λ is necessary in determining the cell size and time-step in the DSMC method. The mean free path for the VHS model is given by

$$\lambda = \frac{8(3 - 2/\alpha)(2 - 2/\alpha)}{15\sqrt{\pi}}\frac{\mu_0}{mn\sqrt{2RT_0}}\left(\frac{T}{T_0}\right)^{2/\alpha}$$

where $R\,(=k/m)$ is the gas constant per unit mass and μ_0 is the viscosity at temperature T_0. In case of $\alpha \to \infty$, we have $\lambda = (16/5)\mu_0/(mn\sqrt{2\pi RT_0})$, which is the mean free path for a hard-sphere molecule.

The VHS model is extended to the case of a gas mixture [39]. In gas mixtures, collisions between unlike molecules occur. Let us regard (68) as the differential cross section for unlike molecule collision by replacing the coefficient A by A'. Of course, A' is assumed to be constant. Then, the mutual diffusion coefficient for species A and B can be obtained as

$$D = \frac{3}{32\sqrt{\pi}\Gamma(3 - 2/\alpha)nA'}\left(\frac{2kT}{\mu_{AB}}\right)^\eta\tag{70}$$

where $n = n_A + n_B$ and $\mu_{AB} = m_Am_B/(m_A + m_B)$ is the reduced mass. The measurements of the temperature dependence of D give the value of the index η. We can also use the measured data of D at the standard condition to determine A'; for example, in a mixture of He and Ar, we have $D = 0.641$ cm^2/s at $n = 2.687 \times 10^{19}$ cm^{-3} and $T = 273$ K [40].

Once A (or A') is determined, the total collision cross section is simply given by

$$\sigma_T = 4\pi A g^{-4/\alpha}. \tag{71}$$

Of course, the postcollision velocities are given by (63a) and (63b).

2) Collision Algorithm for a Simple Gas: Let us consider the molecular collisions in a cell. Let $\boldsymbol{v}_1, \boldsymbol{v}_2, \ldots, \boldsymbol{v}_N$ be the velocities of simulated molecules. The probability P_i that molecule i collides in Δt with some other molecule is given by (62). For a simple gas, it is

$$P_i = \frac{n}{N}\sum_{j=1}^{N} g_{ij}\sigma_T(g_{ij})\Delta t = \sum_{j=1}^{N} P_{ij} \tag{72}$$

where $g_{ij} = |\boldsymbol{v}_i - \boldsymbol{v}_j|$ and

$$P_{ij} = N^{-1}n g_{ij}\sigma_T(g_{ij})\Delta t. \tag{73}$$

Note that $P_{ii} = 0$ because $g_{ii} = 0$. The term for $j = i$ should be omitted in (72). Clearly, P_{ij} is the probability that molecule i collides with molecule j in Δt. The probability P_{ij} is proportional to $g_{ij}\sigma_T(g_{ij})$ or $g_{ij}^{1-4/\alpha}$ for the inverse-power potential; because $\alpha \geq 4$, the probability P_{ij} is an increasing function of g_{ij}. Let us consider a practical upper limit $g_{\max}$ of g_{ij}. The value of $g_{\max}$ can be determined by some sample calculation or can be chosen as $g_{\max} = 5\sqrt{RT_{ref}}$, where T_{ref} is a reference temperature. The latter $g_{\max}$ is 2.5 times the mean relative speed in equilibrium. Skullerud's idea [18] of the null-collision was extended to molecule–molecule collision by Koura [41], Ivanov and Rogasinsky [42], and Yanitskiy [43]. Here, we use the null-collision idea in the simplest way.

If g_{ij} in (73) is replaced by $g_{\max}$, the resulting probability is

$$(P_{ij})_{\max} = N^{-1}n g_{\max}\sigma_T(g_{\max})\Delta t. \tag{74}$$

This probability is greater than P_{ij}. For $P_{ij} = (P_{ij})_{\max}$, (72) takes the form

$$(P_i)_{\max} = nN^{-1}(N-1)g_{\max}\sigma_T(g_{\max})\Delta t.$$

The number of collisions in Δt for $(P_i)_{\max}$ is

$$N_{\max} = \frac{1}{2}\sum_{i=1}^{N}(P_i)_{\max} = \frac{1}{2}n(N-1)g_{\max}\sigma_T(g_{\max})\Delta t. \tag{75}$$

The factor of 1/2 on the right-hand side of (75) is to avoid double counting collisions between like particles. $N_{\max}$ is called the maximum collision number. The computing time necessary to obtain the real collision number

$$N_c = \frac{1}{2}\sum_{i=1}^{N}\sum_{j=1}^{N} P_{ij}$$

is proportional to N^2. This task is formidable because collisions in all cells in a computational domain must be calculated at each time step. In the null-collision method, the task is avoided by regarding $N_{\max}$ as the collision number in Δt. To compensate for excess collisions, $N_{\max} - N_c$, some of the $N_{\max}$ collisions are regarded as null collisions. Let us write

$$P_{ij} = (P_{ij})_{\max}q_{ij} \tag{76}$$

where $q_{ij} = g_{ij}\sigma_T(g_{ij})/g_{\max}\sigma_T(g_{\max})$. Equation (76) can be interpreted as follows. The pair (i, j) first makes a tentative collision with a probability of $(P_{ij})_{\max}$; the tentative collision results in a real collision with a probability of q_{ij} and a null collision with a probability of $1 - q_{ij}$. The number of the tentative collisions is $(P_{ij})_{\max}$ times the number of pairs $N(N-$

$1)/2$; the product is equal to $N_{\max}$. A tentative collision pair can be chosen randomly because $(P_{ij})_{\max}$ is common to all (i, j). Now, let us summarize the method of collision simulation. First, we obtain $N_{\max}$. In general, $N_{\max}$ is not an integer. Let $p = N_{\max} - [N_{\max}]$, where $[N_{\max}]$ is the integral part of $N_{\max}$. We set $N_{\max} = [N_{\max}] + 1$ with a probability of p and $N_{\max} = [N_{\max}]$ with a probability of $1 - p$. We repeat the following two steps $N_{\max}$ times.

1) Choose a pair (i, j) of $i \neq j$ randomly and obtain q_{ij}.
2) Call a random number U. If $U > q_{ij}$, the pair does not collide, and if $U < q_{ij}$, the pair collides. In the latter case, replace the precollision velocities $\boldsymbol{v}_i, \boldsymbol{v}_j$ by the postcollision velocities

$$\boldsymbol{v}_i' = \tfrac{1}{2}(\boldsymbol{v}_i + \boldsymbol{v}_j + g_{ij}\boldsymbol{R}) \tag{77a}$$

$$\boldsymbol{v}_j' = \tfrac{1}{2}(\boldsymbol{v}_i + \boldsymbol{v}_j - g_{ij}\boldsymbol{R}) \tag{77b}$$

where $\boldsymbol{R}$ is a unit vector with a random direction. Note that we assumed the VHS model. A comment is necessary here. The velocities of a collided pair are replaced by the postcollision velocities in step 2); some molecules may collide more than once at the end of the repetitions. This is allowed because the collision algorithm described here is based on the Kac equation [44].

3) Collision Algorithm for a Gas Mixture: The species in plasma reactors are electrons, ions, radicals, and molecules. The velocities of heavy particles are of the same order; heavy particles are treated separately from electrons. Let us consider the collisions among heavy particle species. For the sake of simplicity, we consider a binary mixture of species A and B. The types of collisions are A–A, B–B, and A–B. The A–B collision is a collision between unlike particles. The A–A and B–B collisions are treated as in the case of a simple gas. (If A is a molecule and B is an ion, the B–B collision should be treated separately because it is a Coulomb collision.) Here, we consider only the A–B collision. Let N_A and N_B be the numbers of simulated molecules A and B in a cell. N_A molecules are named $A1$, $A2$, $\ldots$, Ai, $\ldots$, AN_A and N_B molecules are named $B1$, $B2$, $\ldots$, Bj, $\ldots$, BN_B. The probability that molecule Ai collides with some molecule B in Δt is

$$P_{Ai} = n_B \overline{g\sigma_T^{AB}}\Delta t \tag{78}$$

where g is the relative speed and σ_T^{AB} is the total cross section for A–B collision. The average is for all simulated molecules B in a cell; (78) takes the form

$$P_{Ai} = \sum_{j=1}^{N_B} P_{Ai, Bj} \tag{79}$$

where

$$P_{Ai, Bj} = N_B^{-1}n_B g_{Ai, Bj}\sigma_T^{AB}\Delta t. \tag{80}$$

$P_{Ai, Bj}$ is the probability that molecule Ai collides with molecule Bj in Δt. Let us introduce the idea of the maximum collision number. The cross section σ_T^{AB} is a function of $g_{Ai, Bj} = |\boldsymbol{v}_{Ai} - \boldsymbol{v}_{Bj}|$. The factor $g\sigma_T(g)$ increases with g for the inverse-power potential. An estimate of the maximum relative speed, $g_{\max}^{AB}$, is given by $2.5\sqrt{2kT_{ref}/\mu_{AB}}$ as before, μ_{AB}

being the reduced mass. If $g_{Ai, Bj}$ in (80) is replaced by $g_{\max}^{AB}$, we have the upper bound of $P_{Ai, Bj}$

$$P_{\max}^{AB} = N_B^{-1} n_B g_{\max}^{AB} \sigma_T^{AB} \left(g_{\max}^{AB}\right) \Delta t. \tag{81}$$

This equation is the extension of (74) to the case of A–B collision. The maximum number of A–B collisions in Δt for $P_{\max}^{AB}$ is

$$N_{\max}^{AB} = \sum_{i=1}^{N_A} P_{\max}^{AB} = \sum_{i=1}^{N_A} \sum_{j=1}^{N_B} P_{\max}^{AB}. \tag{82}$$

Note that the factor $1/2$ in (75) is not necessary for A–B collisions. Substitution of (81) into (82) yields

$$N_{\max}^{AB} = n_B N_A g_{\max}^{AB} \sigma_T^{AB} \left(g_{\max}^{AB}\right) \Delta t. \tag{83}$$

The number density n_B is expressed as

$$n_B = \frac{W N_B}{V_c} \tag{84}$$

where V_c is the cell volume and W is the weight. One simulated molecule represents W real molecules. In this section, we consider the case when W has a common value for species A and B. Substitution of (84) into (83) shows that $N_{\max}^{AB}$ is unchanged by the interchange of suffixes A and B, as it should be. Equations (83) and (75) can be expressed in a unified form

$$N_{\max}^{sr} = N_s' n_r g_{\max}^{sr} \sigma_T^{sr} \left(g_{\max}^{sr}\right) \Delta t \tag{85}$$

where s, $r = A$ or B, and $N_s' = N_s$ for $s \neq r$ and $N_s' = (N_s - 1)/2$ for $s = r$. The sum of the maximum collision numbers is $N_{\max}^{AA} + N_{\max}^{BB} + N_{\max}^{AB}$.

The procedure of collision simulation based on the VHS model is summarized as follows. The A–A, A–B, and B–B collisions are calculated in turn. The order of the types of collisions is not essential in the calculation. Let us define

$$q_{ij}^{sr} = g_{si, rj} \sigma_T^{sr}(g_{si, rj}) / g_{\max}^{sr} \sigma_T^{sr}(g_{\max}^{sr}).$$

First, repeat steps 1) and 2) $N_{\max}^{AA}$ times.

1) Choose a pair (Ai, Aj) of $i \neq j$ randomly and obtain q_{ij}^{AA}.
2) Call a random number U. If $U > q_{ij}^{AA}$, the pair does not collide, and if $U < q_{ij}^{AA}$, the pair collides, and hence, we replace the precollision velocities by the postcollision velocities in (77a) and (77b).

Secondly, repeat steps 3) and 4) $N_{\max}^{AB}$ times.

3) Choose a pair (Ai, Bj) randomly and obtain q_{ij}^{AB}.
4) Call a random number U. If $U > q_{ij}^{AB}$, the pair does not collide, and if $U < q_{ij}^{AB}$, the pair collides, and hence, we replace the precollision velocities by the postcollision velocities in (63a) and (63b).

Lastly, repeat steps 5) and 6) $N_{\max}^{BB}$ times.

5) Choose a pair (Bi, Bj) of $i \neq j$ randomly and obtain q_{ij}^{BB}.
6) Call a random number U. If $U > q_{ij}^{BB}$, the pair does not collide, and if $U < q_{ij}^{BB}$, the pair collides, and hence, we replace the precollision velocities by the postcollision velocities in (77a) and (77b).

4) Weight Algorithm: In processing plasmas, there may be a large difference among number densities n_A, n_B, n_C, $\ldots$. For example, the density of radicals is often much smaller than is the density of fed gas. If a common weight W is used for all species, a large unbalance appears among the numbers of simulated particles N_A, N_B, N_C, $\ldots$. A smaller number of simulated particles results in a larger fluctuation of sampled flow properties. This inconvenience can be avoided by introducing a smaller weight for species with a lower density [45]. Let W_s be the weight for species s. It is defined by $W_s = n_s V_c / N_s$. See (84). For collisions between like molecules, there is no change in the simulation procedure; (85) for $r = s$ takes the form

$$N_{\max}^{ss} = \tfrac{1}{2} N_s (N_s - 1) W_s V_c^{-1} g_{\max}^{ss} \sigma_T^{ss} \left(g_{\max}^{ss}\right) \Delta t. \tag{86}$$

For collisions between unlike molecules, the difference of weights should be taken into consideration. Let us start from (80). It is rewritten as

$$P_{Ai, Bj} = W_B V_c^{-1} g_{Ai, Bj} \sigma_T^{AB} \Delta t. \tag{87}$$

This is the probability that molecule Ai collides with molecule Bj in Δt. Next, let us consider $P_{Bj, Ai}$. Being similar to (79), the probability that molecule Bj collides with some molecule of species A is

$$P_{Bj} = \sum_{i=1}^{N_A} P_{Bj, Ai}$$

where

$$P_{Bj, Ai} = N_A^{-1} n_A g_{Bj, Ai} \sigma_T^{AB} \Delta t = W_A V_c^{-1} g_{Ai, Bj} \sigma_T^{AB} \Delta t. \tag{88}$$

Note that $g_{Ai, Bj} = g_{Bj, Ai} = |\boldsymbol{v}_{Ai} - \boldsymbol{v}_{Bj}|$. We see that $P_{Ai, Bj} \neq P_{Bj, Ai}$ unless $W_A = W_B$. This is inconvenient; we rewrite (87) and (88) as

$$P_{Ai, Bj} = \frac{W_B}{\max(W_A, W_B)} \cdot q_{ij}^{AB} \cdot P_{\max}^* \tag{89}$$

$$P_{Bj, Ai} = \frac{W_A}{\max(W_A, W_B)} \cdot q_{ij}^{AB} \cdot P_{\max}^* \tag{90}$$

where

$$q_{ij}^{AB} = g_{Ai, Bj} \sigma_T^{AB}(g_{Ai, Bj}) / g_{\max}^{AB} \sigma_T^{AB}(g_{\max}^{AB})$$

and

$$P_{\max}^* = \max(W_A, W_B) V_c^{-1} g_{\max}^{AB} \sigma_T^{AB}(g_{\max}^{AB}) \Delta t. \tag{91}$$

Probability $P_{\max}^*$ is constant and independent of Ai and Bj. Equations (89) and (90) can be interpreted as follows. Let us consider a binary collision of molecules Ai and Bj. The collision can be interpreted by dividing it into three stages. In the first stage, the collision is regarded as occurring with a probability of $P_{\max}^*$. We can determine whether this collision occurs by using one random number. Let us call a realized collision the first tentative collision. In the second stage, the first tentative collision is regarded as true with a probability of q_{ij}^{AB}. We can determine whether the first tentative collision is true or false by using another random number. If the collision is true, we call it the second tentative collision. In the third stage, the second tentative collision is regarded as true with a probability of $W_B / \max(W_A, W_B)$ for molecule Ai and with a probability of $W_A / \max(W_A, W_B)$ for molecule Bj. The number $N_{\max}^*$ of first tentative collisions in a cell is

$$N_{\max}^* = \sum_{i=1}^{N_A} \sum_{j=1}^{N_B} P_{\max}^*$$
$$= \max(N_A, N_B) N_A N_B V_c^{-1} g_{\max}^{AB} \sigma_T^{AB}(g_{\max}^{AB}) \Delta t. \tag{92}$$

We can now summarize the procedure of calculating A–B collisions in Δt in a cell as follows. The VHS model is assumed.

Repeat a set of the following steps 1)–3) $N^*_{\max}$ times.

1) Choose a pair (Ai, Bj) randomly and obtain q^{AB}_{ij}.
2) Call a random number U. If $U > q^{AB}_{ij}$, the pair does not collide, and if $U < q^{AB}_{ij}$, go to step 3).
3) Replace the precollision velocity $\boldsymbol{v}_A$ by the postcollision velocity $\boldsymbol{v}'_A$ with a probability of $W_B/\max(W_A, W_B)$, and replace $\boldsymbol{v}_B$ by $\boldsymbol{v}'_B$ with a probability of $W_A/\max(W_A, W_B)$. The postcollision velocities are in (63a) and (63b).

In step 3) the velocity of the molecule with a smaller weight is always replaced by the postcollision velocity, whereas it is possible that the velocity of the molecule with a larger weight is unchanged. The momentum and energy are not always conserved in collision. But the conservation is satisfied for a system of simulated molecules in a cell when all collisions are taken into consideration. The physical reasoning of step 3) is clear. For example, in the case of $W_A = 1$ and $W_B = 3$, one real molecule A attempts to collide with three real molecules B. Because the collision is binary, however, a molecule A cannot collide with two real molecules B. In other words, one simulated molecule B, which represents three real molecules B, collides with a probability of 1/3.

In closing Section III-C, let us briefly discuss other aspects of the DSMC method. Polyatomic molecules have internal energy in addition to translational energy. Borgnakke and Larsen [46] proposed a method to statistically treat the rotational energy transfer in collision. Boyd [47] extended Borgnakke and Larsen's model to the case when the energy transfer probability depends on the sum of the translational and rotational energies. Matsumoto and Tokumasu [48] proposed a translation–rotation energy transfer model based on real collision dynamics. Reactive collisions can also be simulated if the probability of reaction in collision is given [49]. Two methods to simulate axisymmetrical flows have been proposed: Bird [5] treated molecular motion and collision in the rz-plane, and Riechelmann and Nanbu [50] treated only collision in the rz-plane.

D. Coulomb Collisions

1) Landau–Fokker–Planck Equation: Coulomb collision is a well-known problem of classic mechanics. The collision is called Rutherford scattering. Coulomb collisions in plasma are different from isolated binary collisions. Because the Coulomb force is long range, a moving charged particle receives action from all charged particles within a distance of the Debye length; the Coulomb collision in plasma is in essence a many-body collision. A many-body collision can be treated as a succession of small-angle binary collisions. Based on this idea, Rosenbluth *et al.* [51] starting from the Boltzmann equation, derived the Landau–Fokker–Planck equation for an arbitrary velocity distribution function. Takizuka and Abé [52] proposed a Monte Carlo scheme for simulating the binary collisions in plasmas. Jones *et al.* [53] presented a method to calculate the force acting on a particle from grid quantities in the PIC codes. Their method can be used when deviations of the velocity distribution function from a drifting Maxwellian are small.

Manheimer *et al.* [54] improved the method of Jones *et al.* in such a way that excepting isotropic the velocity distribution is arbitrary. In all of these works, small-angle Coulomb collisions are calculated one by one. If many small-angle collisions can be grouped into one large-angle collision, collisions can be calculated more efficiently because the use of a larger time step is possible. In fact, Cranfill *et al.* [55] used the idea of grouping many small-angle collisions and proposed a time-implicit PIC algorithm. The author [56], [57] proposed a different formulation on a cumulative property of Coulomb collisions in plasmas; he determined the probability distribution for a cumulative deflection angle resulting from many small-angle collisions. The method of collision simulation based on the author's theory is computationally very efficient, although it was obtained on the basis of physical considerations. Bobylev and Nanbu [58] have answered the question of which kinetic equation is solved by this method: Nanbu's method is a solution method of the Landau–Fokker–Planck equation. This equation can be derived from the Boltzmann equation under the assumption of dominant small-angle collisions. In this sense, the collision algorithm described in this section is one for the Landau–Fokker–Planck equation. Here, we start from the Boltzmann equation for a spatially uniform plasma. As was discussed in Section II-A, spatial uniformity can be assumed in constructing collision algorithms provided that the cell size in the simulation is sufficiently small.

Let us consider a plasma composed of s species. Using the Boltzmann equation, Bobylev and Nanbu derived a time-explicit equation that describes the time evolution of a velocity distribution function of species α

$$
\begin{aligned}
&f_\alpha(\boldsymbol{v},\, t + \Delta t) \\
&= \frac{1}{n} \sum_{\beta=1}^{s} \int_{R^3 \times S^2} d\boldsymbol{w}\, d\boldsymbol{\omega} D\left(\frac{\boldsymbol{g} \cdot \boldsymbol{\omega}}{g},\, A_{\alpha\beta} \frac{\Delta t}{g^3}\right) \\
&\quad \cdot f_\alpha\left(\boldsymbol{v}'_{\alpha\beta},\, t\right) f_\beta\left(\boldsymbol{w}'_{\alpha\beta},\, t\right)
\end{aligned}
\tag{93}
$$

where $n\,(=n_1 + n_2 + \cdots + n_s)$ is the total number density; R^3 is 3-D Euclidean space; S^2 is a unit sphere in R^3; $\boldsymbol{g} = \boldsymbol{v} - \boldsymbol{w}$, $\boldsymbol{v}'_{\alpha\beta}$, and $\boldsymbol{w}'_{\alpha\beta}$ are the postcollision velocities

$$
\boldsymbol{v}'_{\alpha\beta} = \boldsymbol{W} + \frac{\mu_{\alpha\beta}}{m_\alpha} g\boldsymbol{\omega}, \quad \boldsymbol{w}'_{\alpha\beta} = \boldsymbol{W} - \frac{\mu_{\alpha\beta}}{m_\beta} g\boldsymbol{\omega}
\tag{94}
$$

$\boldsymbol{W} = (m_\alpha \boldsymbol{v} + m_\beta \boldsymbol{w})/(m_\alpha + m_\beta)$ is the center-of-mass velocity, $\mu_{\alpha\beta} = m_\alpha m_\beta/(m_\alpha + m_\beta)$ is the reduced mass, and

$$
A_{\alpha\beta} = \frac{n}{4\pi} \left(\frac{q_\alpha q_\beta}{\epsilon_0 \mu_{\alpha\beta}}\right)^2 \ln \Lambda_{\alpha\beta}.
\tag{95}
$$

Here, q_α is the charge of particle α, and $\Lambda_{\alpha\beta}$ is given by

$$
\Lambda_{\alpha\beta} = \frac{4\pi\epsilon_0 \mu_{\alpha\beta} \langle g^2_{\alpha\beta}\rangle \lambda_D}{|q_\alpha q_\beta|}
\tag{96}
$$

where λ_D is chosen to be the electron Debye length for any α and β, and $\langle g^2_{\alpha\beta}\rangle$ is the mean square relative velocity between particles α and β. Because the Coulomb logarithm $\ln \Lambda_{\alpha\beta}$ depends weakly on $\Lambda_{\alpha\beta}$, we can approximate $\langle g^2_{\alpha\beta}\rangle$ by using the Maxwellian distributions for species α and β to

$$
\langle g^2_{\alpha\beta}\rangle = \frac{3kT_\alpha}{m_\alpha} + \frac{3kT_\beta}{m_\beta} + \left(\langle \boldsymbol{v}_\alpha\rangle - \langle \boldsymbol{v}_\beta\rangle\right)^2.
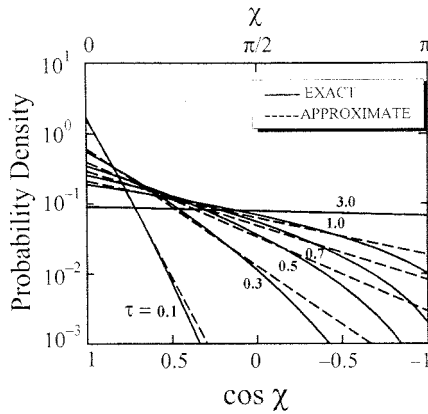$$

Fig. 11.   Exact and approximate probability density functions.

Here, T_α is the temperature and $\langle \boldsymbol{v}_\alpha \rangle$ is the flow velocity. It is important to note that $A_{\alpha\beta} = A_{\beta\alpha}$. The kernel D in (93) is given by

$$D(\mu, \tau) = \sum_{l=0}^{\infty} \frac{2l+1}{4\pi} P_l(\mu) \exp\left[-\frac{1}{2} l(l+1)\tau \right] \quad (97)$$

where $P_l(\mu)$ is the Legendre polynomial. As is seen from (94), $g\boldsymbol{\omega}(= \boldsymbol{v}'_{\alpha\beta} - \boldsymbol{w}'_{\alpha\beta})$ is the postcollision relative velocity, and hence, if χ is the deflection angle, we have $\mu(= \boldsymbol{g} \cdot \boldsymbol{\omega}/g) = \cos\chi$. The function $D(\cos\chi, \tau)$ is the probability density function of $\boldsymbol{\omega}$. From (97), we have

$$2\pi \int_{-1}^{1} P_l(\mu) D(\mu, \tau)\, d\mu = \exp\left[-\tfrac{1}{2}l(l+1)\tau\right] \quad (98)$$

for $l = 0, 1, \ldots$. For $l = 0$, (98) is

$$\int_0^{2\pi} d\psi \int_0^{\pi} D(\cos\chi, \tau) \sin\chi\, d\chi = 1.$$

Clearly, $D(\cos\chi, \tau) \sin\chi\, d\chi\, d\psi$ is the probability that $g\boldsymbol{\omega}$ is directed into $\sin\chi\, d\chi\, d\psi$. It is difficult to obtain a random sample from the complicated function $D(\mu, \tau)$. Let us find an approximation $D^*(\mu, \tau)$ that satisfies (98) only for $l = 0$ and 1. Such a function was obtained from physical considerations [56]

$$D^*(\mu, \tau) = \frac{A}{4\pi \sinh A} \exp(\mu A) \quad (99)$$

with $A = A(\tau)$ satisfying

$$\coth A - A^{-1} = e^\tau. \quad (100)$$

The function $A(\tau)$ was tabulated: $A \simeq \tau^{-1}$ for $\tau < 0.01$ and $A \simeq 3e^{-\tau}$ for $\tau > 3$. Note that $A_{\alpha\beta}\Delta t/g^3$ in the kernel D of (93) corresponds to s in [56]. Fig. 11 shows that (99) is sufficiently accurate for a particle simulation. A random sample μ from $D^*(\mu, \tau)$ is

$$\cos\chi(= \mu) = [A(\tau)]^{-1} \ln\left(e^{-A(\tau)} + 2U \sinh A(\tau) \right) \quad (101)$$

where U is a random number between 0 and 1 and $\tau = A_{\alpha\beta}\Delta t/g^3$.

Coulomb collision algorithms can be derived from (93) by using an expression like (11). First of all, we stress that however small the time step Δt is, all particles collide; the concept of collision probability is not necessary. What is the role of Δt in collision? The role is reflected in the scattering angle χ. As Δt (or $\tau = A_{\alpha\beta}\Delta t/g^3$) decreases, angle χ becomes smaller; (99) shows that $\chi \to 0$ as $\tau \to 0$. This property of Coulomb collision

is different from collisions of short-range forces. Now, let us explain the simplest algorithm for a two-component plasma.

2) Equally Weighted Particles: In the PIC/MC method, computational domain is divided into small cells with a dimension of the Debye length. As in the DSMC method, collisions in each cell can be treated separately from those in other cells. Let us focus our attention on one cell. Let N_α and N_β be the numbers of simulated particles α and β in this cell. The number densities are $n_\alpha = W_\alpha N_\alpha / V_c$ and $n_\beta = W_\beta N_\beta / V_c$, where W_α and W_β are the weights and V_c is the cell volume. First, we consider the case of $W_\alpha = W_\beta = W$. The collision algorithm derived from (93) tells us that the collision partner of particle α is included in species α with a probability of n_α/n and in species β with a probability of n_β/n. Hence, the mean number of particles α colliding with particles β is

$$N'_\alpha = \frac{N_\alpha n_\beta}{n}. \quad (102a)$$

The remaining N''_α is

$$N''_\alpha = N_\alpha - N'_\alpha = \frac{N_\alpha n_\alpha}{n}.$$

This is the mean number of particles α colliding with particles α. Similarly, we can write

$$N'_\beta = \frac{N_\beta n_\alpha}{n} \quad (102b)$$

and $N''_\beta = N_\beta n_\beta / n$, where N'_β represents the mean number of particles β colliding with particles α. The meaning of N''_β may be clear. Although no collision cross section is included in (102a) and (102b), no problem occurs; the concept of collision cross section is included in $A_{\alpha\beta}\Delta t/g^3$ of kernel D in (93). Because $W_\alpha = W_\beta$, we have $N'_\alpha = N'_\beta$. The case of $W_\alpha \neq W_\beta$ is discussed later. Note that because $N'_\alpha + N''_\alpha = N_\alpha$ and $N'_\beta + N''_\beta = N_\beta$, each simulated particle collides only once in Δt, with a like or an unlike particle. The collision algorithm consists of steps 1)–3).

1) Calculate $N'_\alpha (= N'_\beta)$ collisions between particles α and β. Make a random array $(\alpha 1, \alpha 2, \ldots, \alpha N_\alpha)$ of particles α, where αi denotes the ith particle of species α. Similarly, make a random array $(\beta 1, \beta 2, \ldots, \beta N_\beta)$ of particles β. Make N'_α pairs $\{(\alpha i, \beta i): i = 1, 2, \ldots, N'_\alpha\}$, and calculate the collision of each pair. Obtain

$$\tau = \frac{A_{\alpha\beta}\Delta t}{|\boldsymbol{v}_{\alpha i} - \boldsymbol{v}_{\beta i}|^3} \quad (103)$$

and a random sample of $\cos\chi$ from (101). The postcollision velocities are given by (56a) and (56b). To facilitate understanding, we change the notation

$$\boldsymbol{v}'_{\alpha i} = \boldsymbol{v}_{\alpha i} - \frac{m_\beta}{m_\alpha + m_\beta}[\boldsymbol{g}(1 - \cos\chi) + \boldsymbol{h}\sin\chi] \quad (104a)$$

$$\boldsymbol{v}'_{\beta i} = \boldsymbol{v}_{\beta i} + \frac{m_\alpha}{m_\alpha + m_\beta}[\boldsymbol{g}(1 - \cos\chi) + \boldsymbol{h}\sin\chi] \quad (104b)$$

where $\boldsymbol{g} = \boldsymbol{v}_{\alpha i} - \boldsymbol{v}_{\beta i}$ and the Cartesian components of $\boldsymbol{h}$ are

$$h_x = g_\perp \cos\psi$$
$$h_y = -(g_x g_y \cos\psi + g g_z \sin\psi)/g_\perp$$
$$h_z = -(g_x g_z \cos\psi - g g_y \sin\psi)/g_\perp$$

where $g_\perp = (g_y^2 + g_z^2)^{1/2}$. Note that $\sin\chi > 0$ because χ is the polar angle. The angle ψ represents an azimuthal angle of a collision plane. It is given by $\psi = 2\pi U$.

2) The number of particles α that are not used in step 1) is N_α''. These particles are αi's for $i = N_\alpha' + 1, N_\alpha' + 2, \ldots, N_\alpha$. Assume that N_α'' is an even number. The case of an odd number is discussed later. Choose two by two and make $N_p(\equiv N_\alpha''/2)$ pairs. Calculate the collision of each pair. The postcollision velocities are obtained by setting $\beta = \alpha$ in (104a) and (104b).

3) Make $N_p(= N_\beta''/2)$ pairs. Calculate pairwise collisions of particle βj's for $j = N_\alpha' + 1, N_\alpha' + 2, \ldots, N_\beta$, as was done in step 2).

Let us discuss the case when the number N_α'' or N_β'' is odd [59]. As an example, we consider the case of $N_\alpha'' = 5$. Let five particles be $\alpha 5, \alpha 6, \alpha 7, \alpha 8$, and $\alpha 9$. We calculate collisions of three pairs, $(\alpha 5, \alpha 6)$, $(\alpha 7, \alpha 8)$, and $(\alpha 9, \alpha 5')$, where $\alpha 5'$ denotes the second collision of particle $\alpha 5$; namely, the precollision velocity of particle $\alpha 5'$ is the postcollision velocity of particle $\alpha 5$ of the first pair. Clearly, in each collision the physical time of a particle is advanced by Δt. The time increment averaged over N_α'' particles is 3 (pairs) $\times 2\Delta t$ (one pair)/5 = $(6/5)\Delta t$; in general, it is $2\Delta t \times [(N_\alpha'' + 1)/2]/N_\alpha'' = (N_\alpha'' + 1)\Delta t/N_\alpha''$. We write

$$\Delta t_{sys} = \frac{N_\alpha'' + 1}{N_\alpha''}\Delta t. \tag{105}$$

Hence, the average time increment, Δt_{sys}, which is the time increment of a physical system of particles, does not agree with Δt in (103) for $\beta = \alpha$. The time evolution of the particle system should be advanced by a given time step Δt_{sys}. Correction is simple. We have only to shorten Δt in (103) for $\alpha = \beta$ as

$$\tau = \frac{A_{\alpha\alpha}}{|\boldsymbol{v}_{\alpha i} - \boldsymbol{v}_{\alpha j}|^3} \cdot \frac{N_\alpha''}{N_\alpha'' + 1}\Delta t_{sys}. \tag{106}$$

Clearly, the system time is advanced by Δt_{sys} after the collision calculation of $[(N_\alpha'' + 1)/2]$ pairs. In the case of even N_α'', we have $\Delta t_{sys} = \Delta t$, so that the correction factor $N_\alpha''/(N_\alpha'' + 1)$ in (106) is not necessary. The concept of a system time makes it possible to extend the collision algorithm to the case of $W_\alpha \neq W_\beta$.

3) Species-Dependent Weights: In capacitive radiofrequency discharge of chlorine gas, main charged species are electron (α), $Cl^-(\beta)$, and $Cl_2^+(\gamma)$. Except for the sheath near the electrode, charge neutrality is fulfilled: $n_\alpha + n_\beta = n_\gamma$. The electron density n_α is two orders smaller than is the negative ion density n_β. On the other hand, in x-ray laser source plasmas, electron density is much higher than is ion density because all atoms are stripped of all of their electrons. When a large difference exists among species number densities, it is natural to introduce different weights for different species. For the sake of simplicity, we consider a binary mixture of species α and β. Extension to a multicomponent mixture is straightforward. The number densities are $n_\alpha = W_\alpha N_\alpha/V_c$ and $n_\beta = W_\beta N_\beta/V_c$. If $n_\alpha \gg n_\beta$, we introduce the weights proportional to the number densities; thus, we have $N_\alpha \simeq N_\beta$. Equalization of the numbers N_α and N_β of simulated particles is very convenient in particle simulation because equal statistical fluctuations are realized for all species data.

We begin with the meaning of different weights. A collision of simulated particles α and β represents collisions of W_α real particles α and W_β real particles β. Let us consider the

case of $W_\alpha = 5$ and $W_\beta = 3$; only three pairwise collisions can be realized, and hence, two real particles α undergo no collision. This can be described using probability theory; simulated particle α undergoes a collision with a probability of $W_\beta/\max(W_\alpha, W_\beta)[=3/5]$, and simulated particle β does so with a probability of $W_\alpha/\max(W_\alpha, W_\beta)[=1]$. Hence, the postcollision velocities $(\boldsymbol{v}_{\alpha i}^*, \boldsymbol{v}_{\beta i}^*)$ of a pair of simulated particles $(\alpha i, \beta i)$ are given by

$$\boldsymbol{v}_{\alpha i}^* = (1 - Z_\alpha)\boldsymbol{v}_{\alpha i} + Z_\alpha \boldsymbol{v}_{\alpha i}' \tag{107a}$$

$$\boldsymbol{v}_{\beta i}^* = (1 - Z_\beta)\boldsymbol{v}_{\beta i} + Z_\beta \boldsymbol{v}_{\beta i}' \tag{107b}$$

where

$$Prob[Z_\alpha = 1] = W_\beta/\max(W_\alpha, W_\beta) \tag{108a}$$

$$Prob[Z_\alpha = 0] = 1 - Prob[Z_\alpha = 1] \tag{108b}$$

$$Prob[Z_\beta = 1] = W_\alpha/\max(W_\alpha, W_\beta) \tag{108c}$$

$$Prob[Z_\beta = 0] = 1 - Prob[Z_\beta = 1]. \tag{108d}$$

Here, $(\boldsymbol{v}_{\alpha i}', \boldsymbol{v}_{\beta i}')$ are given in (104a) and (104b). Note that in a collision of a pair of simulated particles, the mean number of real particles α that have collided is $W_\alpha \times W_\beta/\max(W_\alpha, W_\beta)$. Similarly, the mean number of real particles β that have collided is $W_\beta \times W_\alpha/\max(W_\alpha, W_\beta)$. The two mean numbers coincide. Now, let us consider the collision algorithm for simulated particles. From (102a) and (102b), we have

$$N_\alpha' = \frac{N_\alpha N_\beta}{nV_c}W_\beta, \qquad N_\beta' = \frac{N_\alpha N_\beta}{nV_c}W_\alpha. \tag{109}$$

We see $N_\alpha' \neq N_\beta'$ for $W_\alpha \neq W_\beta$. Let us consider the case of $N_\alpha' \geq N_\beta'$. As an example, we set $N_\alpha' = 7$ and $N_\beta' = 3$. Let $(\alpha 1, \alpha 2, \ldots, \alpha 7)$ and $(\beta 1, \beta 2, \beta 3)$ be random arrays of particles α and β, respectively. We consider seven collisions. However, we have only three particles β; particles β are let to collide two or three times. The seven collision pairs are $(\alpha 1, \beta 1)$, $(\alpha 2, \beta 2)$, $(\alpha 3, \beta 3)$ for the first collision of particles β, $(\alpha 4, \beta 1')$, $(\alpha 5, \beta 2')$, $(\alpha 6, \beta 3')$ for the second collision, and $(\alpha 7, \beta 1'')$ for the third collision. Here, the precollision velocity of particle $\beta 1'$ is the postcollision velocity of particle $\beta 1$, the precollision velocity of particle $\beta 1''$ is the postcollision velocity of particle $\beta 1'$, and so on. Let us obtain the mean time increment per real particle from this algorithm. It is, for particle α

$$\Delta t \times \frac{W_\alpha W_\beta}{\max(W_\alpha, W_\beta)} \times N_\alpha' \times \frac{1}{W_\alpha N_\alpha'}$$

$$= \frac{W_\beta}{\max(W_\alpha, W_\beta)}\Delta t. \tag{110}$$

For particle β, we have

$$\Delta t \times \frac{W_\alpha W_\beta}{\max(W_\alpha, W_\beta)} \times N_\alpha' \times \frac{1}{W_\beta N_\beta'}$$

$$= \frac{W_\beta}{\max(W_\alpha, W_\beta)}\Delta t$$

where (109) is used. The two time increments agree. Recall that this is the result for $N_\alpha' \geq N_\beta'$, i.e., $W_\beta \geq W_\alpha$ from (109). Therefore, the value of (110) reduces to Δt. The time of a particle system should be advanced by this time increment: we, thus, have $\Delta t_{sys} = \Delta t$. Exchange of suffices α and β shows that $\Delta t_{sys} = \Delta t$ for $N_\alpha' < N_\beta'$ as well.

The collision algorithm for α–α and β–β collisions is the same as that for $W_\alpha = W_\beta$.
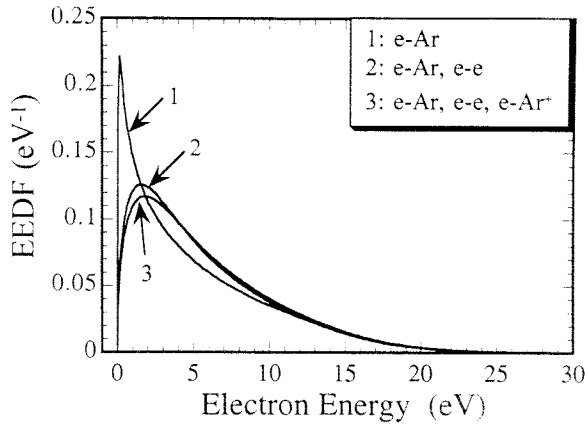
Fig. 12. Electron energy distribution functions obtained by considering 1) e–Ar collisions, 2) e–Ar and e–e collisions, and 3) e–Ar, e–e, and e–Ar$^+$ collisions.

4) Electron Energy Distributions in Inductively Coupled Plasmas: The above algorithm is used to examine the effect of Coulomb collisions on the electron energy distribution in inductively coupled plasmas [60]. Argon gas in an infinitely long tube of quartz glass with a diameter of 20 cm is driven by an RF current (13.56 MHz) in a coil (15 turns/m) wound around the tube wall. The effect of Coulomb collisions is larger for smaller coil current: as the coil current decreases, electron temperature T_e becomes lower, and hence, the average relative velocity g for electron–electron collisions decreases, which results in a larger scattering angle because $\tau = A_{\alpha\alpha}\Delta t/g^3$. The data for the lowest current (3.5 A) are given here. Gas pressure is 5 mTorr, and electron density is 10^{11} cm^{-3}. Three kinds of data are obtained by calculating:

1) e–Ar collisions;
2) e–Ar and e–e collisions;
3) e–Ar, e–e, and e–Ar$^+$ collisions.

In the three cases, electrons lose energy only by e–Ar inelastic collisions. For e–Ar collisions, all collisional events in Fig. 4 are taken into consideration. The motion and collision of electrons in the electromagnetic field are calculated. However, ion velocities are sampled from the Maxwellian distribution with a temperature of 500 K. The ion density is set to be equal to the electron density. Fig. 12 shows the electron energy distribution function (EEDF). We see that e–e collisions greatly influence the EEDF. The effect of e–Ar$^+$ collisions is small but nonnegligible.

E. Charge-Neutralizing Collision of Positive and Negative Ions

In the capacitively coupled radiofrequency discharge of electronegative gas, the electric field in two sheaths confines negative ions in a bulk plasma; positive–negative charge neutralizing collisions are the dominant mechanism for the loss of negative ions. A particle simulation method for charge neutralization has been proposed by Nanbu and Denpoh [61].

Let us consider the reaction

$$A^- + B^+ \rightarrow A + B. \tag{111}$$
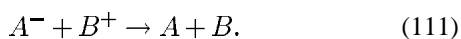
The rate constant $k_r(T)$ for this reaction increases with decreasing temperature T. Here, we consider the case

$$k_r(T) = k_0 \left(\frac{T_0}{T}\right)^n$$

where $0 \leq n \leq 1$ and k_0 is the rate constant at a reference temperature T_0. The index n is, e.g., 0.5 for $O^- + O_2^+ \rightarrow O + O_2$, $O^- + O^+ \rightarrow 2O$, $O_2^- + O_2^+ \rightarrow 2O_2$, and zero for $O^- + O_2^+ \rightarrow 3O$ [62]. The relation between the rate constant $k_r(T)$ and the reaction cross section $\sigma_r(g)$ is

$$
\begin{aligned}
k_r(T) &= \overline{g\sigma_r(g)} \\
&= \left(\frac{\mu_{AB}}{2\pi kT}\right)^{3/2} \int_0^\infty g\sigma_r(g) \exp\left(-\frac{\mu_{AB}g^2}{2kT}\right) 4\pi g^2 \, dg
\end{aligned}
\tag{112}
$$

where g is the relative speed between A^- and B^+ and μ_{AB} is the reduced mass. If we change the integration variable from g to g^2, we see that the right-hand side of (112) has the form of the Laplace transform. The inverse transform yields

$$\sigma_r(g) = \frac{\sqrt{\pi}}{2\Gamma(3/2 - n)} k_0 \left(\frac{2kT_0}{\mu_{AB}}\right)^n g^{-(1+2n)}. \tag{113}$$

Let us consider the cases of $n = 0$ and $1/2$. We have

$$\sigma_r(g) = k_0 g^{-1}, \qquad (n = 0) \tag{114}$$

$$\sigma_r(g) = k_0 \sqrt{\frac{\pi kT_0}{2\mu_{AB}}} g^{-2}. \qquad \left(n = \frac{1}{2}\right). \tag{115}$$

The reactive collision (111) can be considered in the frame of DSMC because (114) and (115) have the form of (68). But some change is necessary because $g\sigma_r(g)$ is now a decreasing function of g. We focus on a cell in a computational domain. Let N_A and N_B be the number of simulated ions A^- and that of B^+ in a cell, respectively, and $\{Ai; i = 1, 2, \ldots, N_A\}$ and $\{Bj; j = 1, 2, \ldots, N_B\}$ be the names of simulated ions. Equations (79) and (80) hold by replacing σ_T^{AB} by σ_r. First, we consider the case of (114). Equation (80) becomes

$$P_{Ai, Bj} = N_B^{-1} n_B k_0 \Delta t. \tag{116}$$

This is independent of pair (Ai, Bj). Therefore, the number of A^-–B^+ reactive collisions in Δt is

$$
\begin{aligned}
N_r &= \sum_{i=1}^{N_A} P_{Ai} \\
&= \sum_{i=1}^{N_A} \sum_{j=1}^{N_B} P_{Ai, Bj} \\
&= N_A n_B k_0 \Delta t = W \frac{N_A N_B}{V_c} k_0 \Delta t
\end{aligned}
\tag{117}
$$

where V_c is the cell volume and W is the weight common to A^- and B^+. The simulation procedure is now clear. Because (116) is independent of relative speed g, we randomly choose N_r pairs (A^-, B^+) of simulated ions and let them become neutral molecules A and B. The velocities $\boldsymbol{v}'_A$, $\boldsymbol{v}'_B$ of the molecules
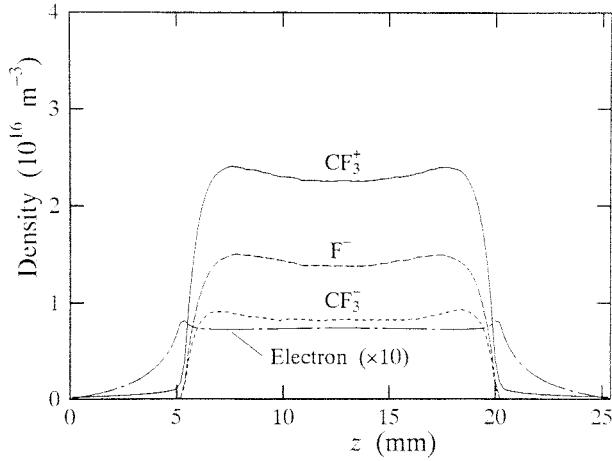
Fig. 13. Number densities of ions and electron.

are given by (63a) and (63b), where $\boldsymbol{v}_A$ and $\boldsymbol{v}_B$ are the ion velocities

Next, we consider the case of (115). This time we have

$$P_{Ai, Bj} = N_B^{-1} n_B k_0 \sqrt{\frac{\pi k T_0}{2\mu_{AB}}} g_{Ai, Bj}^{-1} \Delta t. \tag{118}$$

Again, we can use the idea of the maximum collision number. Note, however, that the probability $P_{Ai, Bj}$ increases with *decreasing* $g_{Ai, Bj}$. We consider a practical *lower* limit $g_{\min}$ of the relative speed. The value of $g_{\min}$ may be chosen as $g_{\min} = 0.1\overline{g}$, where the mean relative speed $\overline{g}$ between A^- and B^+ can be estimated from $(8kT/\pi\mu_{AB})^{1/2}$, T being the ion temperature in a cell. If $g_{Ai, Bj}$ is replaced by $g_{\min}$ in (118), we have the maximum probability

$$P_{\max} = N_B^{-1} n_B k_{\max} \Delta t \tag{119}$$

where $k_{\max} = k_0(\pi k T_0/2\mu_{AB})^{1/2} g_{\min}^{-1}$. As in the case of (83), the maximum number of A^-–B^+ reactive collisions for $P_{\max}$ is

$$N_{\max}^{AB} = W \frac{N_A N_B}{V_c} k_{\max} \Delta t. \tag{120}$$

The maximum collision number method is as follows. Randomly choose $N_{\max}^{AB}$ pairs (Ai, Bj) of simulated ions, and let each of them become neutral molecules with a probability of $P_{Ai, Bj}/P_{\max} (= g_{\min}/g_{Ai, Bj})$. When the charge neutralization occurs, the velocities of molecules A and B are given by (63a) and (63b).

The method described is applied to 1-D radiofrequency discharge of CF_4 [63]. The charged species are electron, positive ions (CF_3^+, CF_2^+, CF^+, C^+, F^+), and negative ions (CF_3^-, F^-). The rate constant of Haverlag *et al.* [64] is used. Fig. 13 shows the number densities of CF_3^+, F^-, CF_3^-, and electron as a function of the distance z normal to the electrode. Other species are negligibly small. The electron density is increased tenfold. The data is obtained for the electrode distance of 25.4 mm, gas pressure of 200 mTorr, secondary electron emission coefficient of 0.1, applied voltage amplitude of 200 V, and driving frequency of 13.56 MHz. The data agree qualitatively with the measurements carried out under some different operating conditions [65], [66].

REFERENCES

[1] C. K. Birdsall, E. Kawamura, and V. Vahedi, "Progress in speeding up a PIC-MCC codes applied to rf plasma discharges," Tohoku Univ., Sendai, Japan, Rep. Inst. Fluid Sci., vol. 10, 1997, pp. 39–47.

[2] C. K. Birdsall and A. B. Langdon, *Plasma Physics via Computer Simulation.* New York: McGraw-Hill, 1985.

[3] R. W. Hockney and J. W. Eastwood, *Computer Simulation Using Particles.* Bristol, U.K.: Inst. of Phys. Publishing, 1988.

[4] C. K. Birdsall, "Particle-in-cell charged-particle simulations, plus Monte Carlo collisions with neutral atoms, PIC-MCC," *IEEE Trans. Plasma Sci.*, vol. 19, pp. 65–85, 1991.

[5] G. A. Bird, *Molecular Gas Dynamics.* Oxford, U.K.: Clarendon Press, 1976.

[6] ——, *Molecular Gas Dynamics and Direct Simulation of Gas Flows.* Oxford, U.K.: Clarendon Press, 1994.

[7] K. Nanbu, "Stochastic theory of motion and collision of charged particle in a uniform electric field," *J. Phys. Soc. Jpn.*, vol. 63, pp. 979–983, 1994.

[8] ——, "Direct simulation scheme derived from the Boltzmann equation.—II. Multicomponent gas mixtures," *J. Phys. Soc. Jpn.*, vol. 49, pp. 2050–2054, 1980.

[9] ——, "Direct simulation scheme derived from the Boltzmann equation—I: Monocomponent gases," *J. Phys. Soc. Jpn.*, vol. 49, pp. 2042–2049, 1980.

[10] H. Babovsky and R. Illner, "A convergence proof for Nanbu's simulation method for the full Boltzmann equation," *SIAM J. Num. Anal.*, vol. 26, pp. 45–65, 1989.

[11] M. N. Rosenbluth, W. M. MacDonald, and D. L. Judd, "Fokker-Planck equation for inverse-square force," *Phys. Rev.*, vol. 107, pp. 1–6, 1957.

[12] A. Date, K. Kitamori, Y. Sakai, and H. Tagashira, "Self-consistent Monte Carlo modeling of rf plasma in a helium-like model gas," *J. Phys. D: Appl. Phys.*, vol. 25, pp. 442–452, 1992.

[13] D. P. Lymberopoulos and D. J. Economou, "Spatiotemporal electron dynamics in radio-frequency glow discharges: fluid versus dynamic Monte Carlo simulations," *J. Phys. D: Appl. Phys.*, vol. 28, pp. 727–737, 1995.

[14] K. Nanbu and Y. Kitatani, "Self-consistent particle simulation of rf discharge in argon based on detailed collision data," *Vacuum*, vol. 47, pp. 1023–1025, 1996.

[15] K. Nanbu and J. Kageyama, "Detailed structure of dc glow discharges-effects of pressure, applied voltage, and γ-coefficient," *Vacuum*, vol. 47, pp. 1031–1033, 1996.

[16] K. Nanbu and S. Kondo, "Analysis of three-dimensional dc magnetron discharge by the particle-in-cell/Monte Carlo method," *Jpn. J. Appl. Phys.*, vol. 36, pp. 4808–4814, 1997.

[17] S. Kondo and K. Nanbu, "Chaotic dynamics of three-dimensional dc magnetron discharge," *IEEE Trans. Plasma Sci.*, vol. 27, pp. 92–93, 1999.

[18] H. R. Skullerud, "The stochastic computer simulating of ion motion in a gas subject to a constant electric field," *Brit. J. Appl. Phys.*, ser. 2, vol. 1, pp. 1567–1568, 1968.

[19] K. Nanbu, "Simple method to determine collisional event in Monte Carlo simulation of electron–molecule collision," *Jpn. J. Appl. Phys.*, vol. 33, pp. 4752–4753, 1994.

[20] K. Kosaki and M. Hayashi, "Electron–argon atom collision cross sections" (in Japanese), in Preprint Nat. Mtg. Inst. Elect. Eng., 1992, to be published.

[21] L. R. Peterson and J. E. Allen Jr., "Electron impact cross sections for argon," *J. Chem. Phys.*, vol. 56, pp. 6068–6076, 1972.

[22] M. Surendra, D. B. Graves, and G. M. Jellum, "Self-consistent model of a direct current glow discharge: Treatment of fast electrons," *Phys. Rev. A.*, vol. 41, pp. 1112–1125, 1990.

[23] W. G. Vincenti and C. H. Kruger Jr., *Introduction to Physical Gas Dynamics.* New York, NY: Wiley, 1967, pp. 352–353.

[24] Y. Nakamura and M. Kurachi, "Electron transport parameters in argon and its momentum transfer cross section," *J. Phys. D: Appl. Phys.*, vol. 21, pp. 718–723, 1988.

[25] A. V. Phelps.. [Online]ftp://jila.colorado.edu/collision_data/eletrans.txt

[26] L. G. Christophorou and J. K. Olthoff, "Electron interactions with Cl_2," *J. Phys. Chem. Ref. Data*, vol. 28, pp. 131–169, 1999.

[27] W. L. Morgan, "A critical evaluation of low-energy electron impact cross sections for plasma processing modeling. I: Cl_2, F_2, and HCl," *Plasma Chem. Plasma Processing*, vol. 12, pp. 449–476, 1992.

[28] T. N. Rescigno, "Low-energy electron collision processes in molecular chlorine," *Phys. Rev. A.*, vol. 50, pp. 1382–1389, 1994.

[29] M. Gote and H. Ehrhardt, "Rotational excitation of diatomic molecules at intermediate energies: Absolute differential state-to-state transition cross sections for electron scattering for N_2, Cl_2, CO and HCl," *J. Phys. B*, vol. 28, pp. 3957–3986, 1995.

[30] W. L. Morgan, private communication.

[31] K. Nanbu, T. Morimoto, and S. Igarashi, "Growth rate of films fabricated by the sputtering method," in *Rarefied Gas Dynamics*, A. E. Beylich, ed. Weinheim, Germany: VCH, 1991, pp. 913–920.

[32] E. A. Mason and E. W. McDaniel, *Transport Properties of Ions in Gases*. New York: Wiley, 1988, p. 326.

[33] K. Nanbu and G. Wakayama, "A simple model for Ar^+–Ar, He^+–He, Ne^+–Ne and Kr^+–Kr collisions," *Jpn. J. Appl. Phys.*, vol. 38, pp. 6097–6099, 1999.

[34] S. Chapman and T. G. Cowling, *The Mathematical Theory of Non-Uniform Gases*, 3rd ed. London: Cambridge Univ. Press, 1970, p. 228.

[35] H. W. Ellis, R. Y. Pai, E. W. McDaniel, E. A. Mason, and L. A. Viehland, "Transport properties of gaseous ions over a wide energy range," *Atom. Data Nucl. Data Tables*, vol. 17, pp. 177–210, 1976.

[36] L. A. Viehland and E. A. Mason, "Transport properties of gaseous ions over a wide energy range, IV," *Atom. Data Nucl. Data Tables*, vol. 60, pp. 37–95, 1995.

[37] K. Nanbu and Y. Kitatani, "An ion–neutral species collision model for particle simulation of glow discharge," *J. Phys. D: Appl. Phys.*, vol. 28, pp. 324–330, 1995.

[38] W. G. Vincenti and C. H. Kruger Jr., *Introduction to Physical Gas Dynamics*. New York: Wiley, 1967, p. 404.

[39] K. Nanbu, "Variable hard-sphere model for gas mixture," *J. Phys. Soc. Jpn.*, vol. 59, pp. 4331–4333, 1990.

[40] S. Chapman and T. G. Cowling, *The Mathematical Theory of Non-Uniform Gases*, 3rd ed. London: Cambridge Univ. Press, 1970, p. 263.

[41] K. Koura, "Null-collision technique in the direct-simulation Monte Carlo method," *Phys. Fluids*, vol. 29, pp. 3509–3511, 1986.

[42] M. S. Ivanov and S. V. Rogasinsky, "Analysis of numerical techniques of the direct simulation Monte Carlo method in the rarefied gas dynamics," *Sov. J. Numer. Anal. Math. Modeling*, vol. 3, pp. 453–465, 1988.

[43] V. E. Yanitskiy, "Operator approach to direct Monte Carlo simulation theory in rarefied gas dynamics," in *Rarefied Gas Dynamics*, A. E. Beylich, ed. Weinheim, Germany: VCH, 1991, pp. 770–777.

[44] K. Nanbu, "Theoretical basis of the direct simulation Monte Carlo method," in *Proc. Int. Symp. Rarefied Gas Dynamics*, vol. 1, V. Boffi and C. Cercignani, Eds. Stuttgard, Germany, 1986, pp. 369–383.

[45] V. E. Yanitskiy and V. V. Serikov, "Multicomponent rarefied gas weighting algorithms for Monte Carlo simulation," in *Proc. 2nd Jpn.-Soviet Union Joint Symp. Computat. Fluid Dynamics*, vol. 2, Y. Yoshizawa and K. Oshima, Eds. Tsukuba, Japan, 1990, pp. 36–43.

[46] C. Borgnakke and P. S. Larsen, "Statistical collision model for Monte Carlo simulation of polyatomic gas mixture," *J. Comput. Phys.*, vol. 18, pp. 405–420, 1975.

[47] I. D. Boyd, "Analysis of rotational nonequilibrium in standing shock waves of nitrogen," *AIAA J.*, vol. 28, pp. 1997–1999, 1997.

[48] Y. Matsumoto and T. Tokumasu, "Collision model of diatomic molecules for DSMC method," in *Rarefied Gas Dynamics*, J. Harvey and G. Lord, Eds. Oxford, U.K.: Oxford Univ. Press, 1995, pp. 808–814.

[49] K. Nanbu, *Stochastic solution method of the Boltzmann equation—II. Simple gas, gas mixture, diatomic gas, reactive gas, and plasma*, Japan: Rep. Inst. Fluid Science, Tohoku Univ., 1996, vol. 8, pp. 77–125.

[50] D. Riechelmann and K. Nanbu, "Monte Carlo direct simulation of the Taylor instability in rarefied gas," *Phys. Fluids A*, vol. 5, pp. 2585–2587, 1993.

[51] M. N. Rosenbluth, W. M. MacDonald, and D. L. Judd, "Fokker-Planck equation for inverse square force," *Phys. Rev.*, vol. 107, pp. 1–6, 1957.

[52] T. Takizuka and H. Abé, "A binary collision model for plasma simulation with a particle code," *J. Comput. Phys.*, vol. 25, pp. 205–219, 1977.

[53] M. E. Jones, D. S. Lemons, R. J. Mason, V. A. Thomas, and D. Winske, "A grid-based Coulomb collision model for PIC codes," *J. Comput. Phys.*, vol. 123, pp. 169–181, 1996.

[54] W. M. Manheimer, M. Lampe, and G. Joyce, "Langevin representation of Coulomb collisions in PIC simulations," *J. Comput. Phys.*, vol. 138, pp. 563–584, 1997.

[55] C. W. Cranfill, J. U. Brackbill, and S. R. Goldman, "A time-implicit Monte Carlo collision algorithm for particle-in-cell electron transport models," *J. Comput. Phys.*, vol. 66, pp. 239–249, 1986.

[56] K. Nanbu, "Theory of cumulative small-angle collisions in plasmas," *Phys. Rev. E*, vol. 55, pp. 4642–4652, 1997.

[57] ——, "Momentum relaxation of a charged particle by small-angle Coulomb collisions," *Phys. Rev. E*, vol. 56, p. 7314, 1997.

[58] A. V. Bobylev and K. Nanbu, "Theory of collision algorithms for gases and plasmas based on the Boltzmann equation and Landau–Fokker–Planck equation," *Phys. Rev. E*, vol. 61, pp. 4576–4586, 2000.

[59] K. Nanbu and S. Yonemura, "Weighted particles in Coulomb collision simulations based on the theory of a cumulative scattering angle," *J. Comput. Phys.*, vol. 145, pp. 639–654, 1998.

[60] S. Yonemura, K. Nanbu, T. Morimoto, and K. Sakai, "Electron energy distributions in an inductively coupled plasma reactor," in *Proc. 21st Int. Symp. Rarefied Gas Dynamics*, R. Brun, R. Campargue, R. Gatignol, and J.-C. Lengrand, Eds, Toulouse, France: Cépaduès-Éditions, 1999, vol. 2, pp. 39–46.

[61] K. Nanbu and K. Denpoh, "Monte Carlo collision simulation of positive–negative ion recombination for a given rate constant," *J. Phys. Soc. Jpn.*, vol. 67, pp. 1288–1290, 1998.

[62] M. A. Lieberman and A. J. Lichtenberg, *Principles of Plasma Discharges and Materials Processing*. New York, NY: Wiley, 1994, p. 238.

[63] K. Denpoh and K. Nanbu, "Self-consistent particle simulation of radio-frequency CF_4 discharges with implementation of all ion–neutral reactive collisions," *J. Vac. Sci. Technol. A*, vol. 16, pp. 1201–1206, 1998.

[64] M. Harverlag, A. Kono, D. Passchier, G. M. W. Kroesen, W. J. Goedheer, and F. J. de Hoog, "Measurements of negative ion densities in 13.56-MHz rf plasmas of CF_4, C_2F_6, CHF_3, and C_3F_8 using microwave resonance and the photodetachment effect," *J. Appl. Phys.*, vol. 70, pp. 3472–3480, 1991.

[65] I. Iga, M. V. V. S. Rao, S. K. Srivastava, and J. C. Nogueira, "Formation of negative ions by electron impact on SiF_4 and CF_4," *Z. Phys. D—Atoms, Molecules and Clusters*, vol. 24, pp. 111–115, 1992.

[66] K. Stephan, H. Deutsch, and T. D. Märk, "Absolute partial and total electron impact ionization cross sections for CF_4 from threshold up to 180 eV," *J. Chem. Phys.*, vol. 83, pp. 5712–5720, 1985.

Kenichi Nanbu (M'99) was born in Japan on February 22, 1943. He received the B.E. degree in 1965 from Kanazawa University, Japan, and the M.E. and D.E. degrees in 1967 and 1970, respectively, from Tohoku University, Sendai, Japan.

He was a Lecturer in 1970, an Associate Professor in 1974, and a Professor in 1986 at Tohoku University. He is a Professor in the Institute of Fluid Science, Tohoku University. His work has concentrated on stochastic modeling of collision processes in rarefied gas and plasma, particularly in the study of materials processing. His papers can be found at http://www.ifs.tohoku.ac.jp.